



# Reviews and syntheses: Eddy covariance-based evapotranspiration partitioning

Emma G. Cochran<sup>1</sup>, Claudia Wagner-Riddle<sup>2</sup>, Elke Eichelmann<sup>1</sup>

<sup>1</sup>School of Biology and Environmental Science, University College Dublin, Belfield, Dublin 4, Ireland

5 <sup>2</sup>School of Environmental Sciences, University of Guelph, Guelph, Ontario, Canada

*Correspondence to:* Emma G. Cochran (cochranemma17@gmail.com)

**Abstract.** The task of reliably partitioning evapotranspiration (ET) is imperative so that we can better understand how individual components of the terrestrial water flux are contributing to the global hydrological cycle and changing under a warming climate. By constraining how evaporation (E) and transpiration (T) separately adapt to increased global temperatures, we can make more accurate predictions in land surface models, further our understanding of plant water use, and better manage our limited water resources. Eddy covariance (EC) is a globally used technique that measures net biosphere-atmosphere fluxes, including ET, and if reliably partitioned, presents a promising way to constrain E and T values and trends across ecosystems. Several EC-based ET partitioning methods exist, and there is a need for an updated comprehensive guide to the available approaches. This systematic literature review was conducted with the objectives of 1) identifying EC-based ET partitioning methods and categorizing them based on underlying ecosystem assumptions, 2) determining the main advantages and disadvantages of each method dependent on their assumptions and data requirements, and 3) evaluating how broadly these methods have been tested based on geographic location and ecosystem type. The review identified 10 independent partitioning methods tested across 123 studies. Methods using assumptions of underlying water use efficiency (uWUE) and ecosystem conductance all use the relationship between ET and gross primary production with vapor pressure deficit (VPD) to estimate the transpiration ratio (T/ET). Additionally, two machine learning based methods, one method assuming a linear relationship between ET and gross ecosystem photosynthesis, and three methods using high frequency EC data to estimate T/ET were identified. The uWUE methods, while the most frequently used partitioning approach, consistently predicted the lowest T/ET estimates when compared to both other EC and non-EC based partitioning methods. The machine learning methods predicted the highest T/ET values compared to other EC-based methods which agreed well with values estimated with independent methods. Savannas and evergreen broadleaf forests had the highest T/ET of all ecosystem types while deserts and wetlands had the lowest. Leaf area index and soil water content were found to be the most important drivers of T/ET values and trends with VPD and air temperature also displaying significant effects. Of the global studies identified in this review, an average annual T/ET value of 0.58 was found, a value that falls within the range of other studies using isotopic partitioning, remote sensing methods, and global estimates from various ecosystem models. More testing, specifically increased paired analyses of two or more EC-based ET partitioning methods on the same dataset, is needed in order to fully understand the applicability of each method, their differences, and to better constrain global T/ET dynamics.



## 1 Introduction

Evapotranspiration (ET) is the combined water flux of terrestrial ecosystems whereby 65,000 – 76,000 km<sup>3</sup> of water leaves land surfaces to the atmosphere annually (Dorigo et al., 2021; Jung et al., 2019; Oki & Kanae, 2006). While global ET trends will continue to change under the warming climate, land surface models (LSM) have not converged on a predicted trend with some models indicating an increase in global ET due to increased temperatures (Brutsaert, 2017; Zeng et al., 2018) and other models indicating a decrease due to decreased water supply (Gedney et al., 2006; Jung et al., 2010). The importance of properly constraining the water flux in LSMs is paramount so that we can further our understanding of the terrestrial water cycle and better manage water resources under a changing climate (Dolman et al., 2014; Fisher et al., 2017; Stoy et al., 2019). However, to reliably model and predict ET, we must understand its two primary components: evaporation (E) and transpiration (T).

Evaporation is a physical process by which water is lost from non-stomatal surfaces, often soil surfaces (bare soil evaporation) or a wet canopy (interception evaporation). Water availability and vapor pressure deficit (VPD) are major drivers of E where the magnitude of E increases when atmospheric water demand and the surface soil water content are high (Kool et al., 2014; Scott & Biederman, 2017). Transpiration is water lost through stomata during carbon assimilation, linking the carbon and water fluxes from vascular plants (Katul et al., 2012; Kool et al., 2014; Li et al., 2019; Zhou et al., 2016). T is the other major component of ET, but has large uncertainties on a global scale, accounting for anywhere from 35-90% of the annual water flux from land surfaces (Coenders-Gerritis et al., 2014; Good et al., 2015; Jasechko et al., 2013; Schlesinger & Jasechko, 2014; Wang et al., 2014). T is largely dependent on leaf physiology and is difficult to estimate in heterogenous ecosystems (Nelson et al., 2020; Reich et al., 2024). Like E, T is also dependent on soil water availability and VPD (Beer et al., 2009; Grossiord et al., 2020; López et al., 2021b). T is predicted to increase with rising global VPD, leading to a decrease in plant water use efficiency (López et al., 2021b; Novick et al., 2016; Yuan et al., 2019) although this response is highly variable depending on plant species and environmental conditions (Grossiord et al., 2020). Because T is a major component of the terrestrial water flux, its shifts in magnitude due to climate change will have repercussions for the rest of the global water cycle (Berkelhammer et al., 2016; Gerken et al., 2018).

While both T and E have similar and even overlapping drivers, the rates at which they respond to these drivers are unequal in magnitude (Scott & Biederman, 2017). For example, the timescales on which E and T operate differ significantly, another factor impacting the hydrological cycle (Scott et al., 2006; Scott & Biederman, 2017). Rates of E will increase in response to any precipitation event that results in wet surfaces. On the other hand, T will only respond to rainfall when enough water has entered the ecosystem and root zone to allow for plant water uptake, a response that can lag up to 10 days after the precipitation event (Kurc & Small, 2007; Scott et al., 2006). Perhaps the biggest difference in the drivers of T and E is that T is significantly affected by vegetation type and plant water dynamics, while E is only dependent on environmental conditions (Wang et al., 2014; Zhou et al., 2016). This makes T an active, biotic process regulated by stomatal conductance, while E remains a passive, abiotic process (Nelson et al., 2018) and the differentiation of the biotic and abiotic components of ET will allow for the study of how the water cycle is impacted by changes in vegetation (Cao et al., 2010; Scott & Biederman, 2017;



65 Wilcox et al., 2012). By quantifying the relative contributions of T and E, we can also study the influences of changing climatic and biological conditions on the spatial and temporal variability of ET (Gan & Liu, 2020; Reich et al., 2024).

Direct measurements of T or E by means of isotopic, sap-flux, or soil evaporation methods are time, money, and labor intensive and are associated with significant uncertainties when upscaling to the ecosystem level (Cammalleri et al., 2013; Griffis, 2013; Kool et al., 2014; Li et al., 2019; Oishi et al., 2008; Poyatos et al., 2016; Stoy et al., 2019; Wilson et al., 2001). Modeling  
70 methods often require complex parameterization and require validation data not easily accessible (Fatichi & Pappas, 2017; Kool et al., 2014; Sun et al., 2018) On the other hand, eddy covariance (EC) is a technique used to measure ecosystem gas and heat exchange within the atmospheric boundary layer, including ET (Baldocchi, 2020). Rather than directly measuring T or E, methods have been developed to partition eddy covariance ET measurements into its relative components. However, while  
75 Taylor) as well as non-EC data-based methods (i.e., solar induced fluorescence-based, carbonyl sulfide flux-based, and isotope-based) (Kool et al., 2014; Stoy et al., 2019) are available, there is a need for an updated, comprehensive review of EC-based partitioning methods.

FLUXNET, a collaboration of EC networks, provides open-source, public micrometeorological data from hundreds of ecosystems under various climates which can be used to create spatial maps of global carbon and water fluxes (Baldocchi,  
80 2020; Pastorello et al., 2020; Williams et al., 2009). Because of this, FLUXNET data is often used as ground truth to validate and parameterize remote sensing data products and LSMs. Therefore, partitioned E and T data derived from EC ecosystem water data, would improve LSMs' prediction capabilities (Bonan et al., 2011, 2012; Chaney et al., 2016; Friend et al., 2007; Kool et al., 2014; Nogueira et al., 2021; Reich et al., 2024; Stapleton et al., 2022; Stoy et al., 2019; Williams et al., 2009). Additionally, the continuous, high-frequency measurements allow for flux analyses ranging from 30 min intervals to  
85 interannual trends, giving researchers key insights into how ecosystem water pathways behave and evolve over time in response to a changing climate (Baldocchi, 2003, 2020; Eichelmann et al., 2022).

Previous work in partitioning the terrestrial ecosystem carbon flux from EC-measured net ecosystem exchange (NEE) into gross primary production (GPP) and ecosystem respiration has led to significant improvements in understanding the interannual variability of NEE across ecosystems (Lasslop et al., 2010; Reichstein et al., 2005). This has furthered our  
90 understanding of global and regional carbon fluxes as well as aided in the study of the role of vegetation as a vital carbon sink (Chatterjee et al., 2020; Stoy et al., 2006). The ability to partition the terrestrial ecosystem water flux from FLUXNET data will have implications of a similar magnitude. Various methods exist to partition EC-measured ET and there is a need to create a comprehensive guide to the available approaches.

Here we reviewed EC-based ET partitioning methods using data routinely collected at flux towers to answer three  
95 questions:

1. What EC-based ET partitioning methods exist and on which ecosystem assumptions are they based?
2. Based on ecosystem assumptions and data availability, what are the main advantages and disadvantages of each method?



3. What is the breadth (geographic location and ecosystem type) of testing of each method?

100 This review, in line with much of current work, presents the transpiration ratio (T/ET) to evaluate partitioning results and includes methods that could be applied on any FLUXNET dataset.

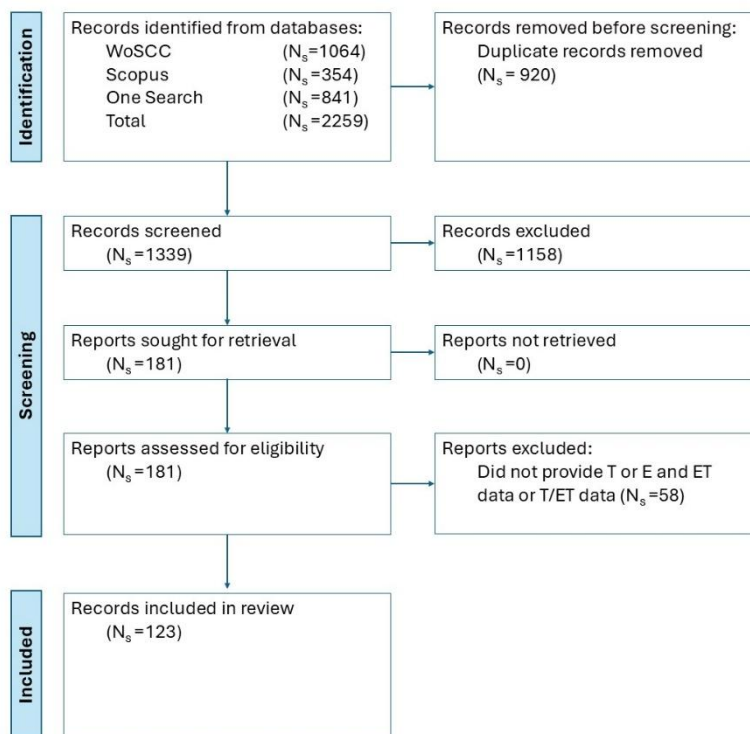
## 2 Methods

A systematic literature review was conducted of ET partitioning methods including studies that reported T and E with ET data or T/ET ratios calculated using data routinely collected from eddy covariance sites. EC-based ET partitioning methods were categorized by underlying principles. Several sub-methods were identified as slight adjustments to previously established methods and are also discussed. The search was conducted using the Web of Science Core Collection (WoSCC), Scopus, and University College Dublin's OneSearch database, a public online database search tool that encompasses hundreds of journals across disciplines. The following key words were used: "evapotranspiration partitioning eddy covariance", "eddy covariance latent heat partitioning", "flux variance similarity evapotranspiration", "eddy covariance transpiration evaporation ratio", and "eddy covariance evapotranspiration components". Additionally, papers that had cited an established partitioning method were identified using WoSCC and screened for eligibility. Only peer reviewed studies published in English were included, excluding theses and conference papers. The databases were last searched on September 25<sup>th</sup>, 2025.

Partitioning methods that use EC data combined with data from other sources (often LAI, remote sensing products, isotopes, or LSMs) were excluded. Data reported in either numerical or graphical formats were included. If the values or trends of T/ET could not be determined from the reported data (often in the case where correlation coefficients or statistical results were reported in terms of how one partitioning method compared to another method), the study was excluded.

Above- and below-canopy concurrent EC measurements can be used to partition ET in forests and woody savannas by assuming the below-canopy system measures soil E (Ma et al., 2020; Paul-Limoges et al., 2020; Sulman et al., 2016; Wilson et al., 2001). However, this method requires dual EC systems across a vertical profile and therefore was excluded from the identified methods as below canopy measurements are not routinely collected.

The resulting studies were then screened by one reviewer with no automation tools. If available, data pertaining to T or E with ET values and/or trends, T/ET values and/or trends, the temporal scale on which the partitioning method was applied, the flux site location (and site i.d. when provided), and plant functional type (PFT) were extracted. If results were provided in both graphical and numerical contexts, the numerical data were included. Supplementary documents were searched in conjunction with the main text of the screened studies and eligible data were extracted in the same way. A total of 1339 papers were identified in the original search, however, only 123 (=N<sub>S</sub>) papers were included in the final review (Fig. 1). The number of records (N<sub>R</sub>) or datasets reported within a study was also recorded. For instance, if a study conducted analyses in 3 different ecosystem types and reported separate T/ET values for each, N<sub>S</sub> would equal 1 while N<sub>R</sub> would equal 3.



130 **Figure 1: PRISMA 2020 flow diagram for systematic reviews** (Page et al., 2021) showing for the review: the databases searched, the number of studies found (N<sub>s</sub>), and the number of studies included in the final review.

### 3 Results

#### 3.1 ET partitioning methods, their assumptions, advantages, and disadvantages

135 Ten independent partitioning methods were identified, each built from a range of ecosystem assumptions. Methods based on the concept of underlying water use efficiency (uWUE) were compared to ecosystem conductance-based methods, machine learning methods, methods requiring high frequency data, and linear regression-based methods (Table 1).

140 Table 1: Summary table of EC-based ET partitioning methods, their data requirements, theory, and main advantages/disadvantages. Independent methods have their own abbreviation while sub-methods are denoted with a ‘b’ and the abbreviation of the method on which they are based. GPP: gross primary production, VPD: vapor pressure deficit, ET: evapotranspiration, uWUE: underlying water use efficiency, LE: latent heat flux, H: sensible heat flux, TA: air temperature, CA: ambient CO<sub>2</sub> mixing ratio, PA: air pressure, U\*: friction velocity, WS: wind speed, ↓K: incoming shortwave radiation, ↓KPOT: potential incoming shortwave radiation, Z: altitude, PAR: photosynthetically active radiation (from the PPF<sub>D</sub>\_IN



145 variable in FLUXNET datasets), P: precipitation, c: CO<sub>2</sub> concentration, q: H<sub>2</sub>O concentration, u: wind speed from the predominate direction, v: cross-stream wind speed, w: vertical wind speed

Method Type	Method	Data Required	Basic Theory	Advantages	Disadvantages	Source
<b>uWUE</b>	ZH16	GPP, VPD, ET	An ecosystem has a potential uWUE (when ET=T) and an actual uWUE which when combined are proportional to T/ET	T/ET estimates from daily to annual timescales, easy implementation	Reliance on GPP estimates, methods assumptions do not hold in heterogenous ecosystems, wetlands, or under low VPD conditions	(Zhou et al., 2016)
	BH16	GPP, VPD, ET	Similar to ZH16, except potential uWUE is determined using binned GPP values	Does not exclude rainy periods, easy implementation	Same as ZH16	(Berkelhammer et al., 2016)
<b>Stomatal conductance</b>	LI19	GPP, VPD, and ET, soil moisture	Parameter optimization to separate surface conductance into its soil and canopy components, which are proportional to T/ET	Takes into account vegetation type, does not assume periods where ET=T	Reliance on GPP estimates, excludes rainy and wet periods, method assumptions do not hold in heterogenous ecosystems or drylands	(Li et al., 2019)
	PP18	GPP, VPD, LE, H, T <sub>A</sub> , C <sub>A</sub> , P <sub>A</sub> , U*, WS, ↓K, Z, PAR	Big-leaf canopy model used to estimate canopy conductance responses to changing environmental conditions	Does not assume periods where ET=T	Same as LI19, often fails to produce reliable T estimates	(Perez-Priego et al., 2018)
<b>Machine learning</b>	TEA18	GPP, VPD, ET, ↓K, ↓K <sub>POT</sub> T <sub>A</sub> , P, WS	Uses a Random Forest regressor to estimate WUE	Captures half hourly patterns of T from minimal	Excludes rainy and wet periods, method	(Nelson et al., 2018)



			when $ET=T$ to be used with GPP to estimate half-hour T	data requirements, low computational power requirements	assumptions not held in ecosystems with significant E contributions	
	EE22	VPD, H, $T_A$ , $U^*$	Uses a neural network to partition daytime ET fluxes assuming nighttime $ET=E$	Does not rely on periods when $T=ET$ , does not use GPP estimates	Requires domain knowledge for feature selection*, assumptions not held in ecosystems with nocturnal transpiration	(Eichelmann et al., 2022)
<b>High frequency</b>	SK10	High frequency c, q, u, v, w	Stomatal (T) and non-stomatal (E) processes independently adhere to flux variance similarity	Open source through Fluxpart, customization in WUE calculation	Requires high frequency data, assumptions not met in heterogenous canopies, often fails to produce reliable T estimates	(Scanlon & Kustas, 2010; Scanlon & Sahu, 2008)
	TH08	High frequency c, q, u, v, w	Similar to SK10 but identifies updrafts where c and q are equal to E	Created for ecosystems with tall, low-density canopies but has been shown to work well in dense canopies**	Requires high frequency data, heavy computational power required	(Thomas et al., 2008)
	TH08b	High frequency c, q, u, v, w	Conditional eddy accumulation method, similar to TH08 but includes downdrafts	Does not require a priori knowledge of WUE	Same as TH08	(Zahn et al., 2024)
	ZN22	High frequency c, q, u, v, w	Conditional eddy covariance method, defines conditional covariances where w and q are proportional to E and T	Does not require a priori knowledge of WUE	Requires high frequency data, heavy computational resources required	(Zahn et al., 2022)



	ZN22b	High frequency c, q, u, v, w, WUE	Same as ZN22 but with the addition of WUE if known to better constrain the carbon flux	Simpler than SK10, allowing for easier implementation	Same as ZN22	(Zahn et al., 2024)
<b>Linear regression</b>	SB17	GPP, ET	T is related to GPP on an interannual basis and can be solved for using a linear regression on monthly timescales	No assumption that ET=T, easy implementation	Ideal datasets of 5-7 years of length (minimum 3 years) limit site applicability, suppresses rainy periods	(Scott & Biederman, 2017)
	SB17b	GPP, ET	Built off of SB17 to estimate weekly WUE and subsequent weekly T	Daily to weekly T estimates improved from monthly estimates from SB17	Not well suited for heterogenous ecosystems	(Reich et al., 2024)

\*This was adjusted for in Stapleton et al., 2022

\*\*From Klosterhalfen et al. (2019a)

### 3.1.1 Underlying water use efficiency

Zhou et al. (2016) established a method (hereafter, ZH16) based on underlying water use efficiency (uWUE) to partition ET based on half-hourly flux data. This method assumes that at sub-daily time scales, periods occur when soil and canopy interception evaporation are negligible and T/ET approaches 1. These conditions are then used to define the potential uWUE (uWUE<sub>p</sub>), a value assumed to be constant over long time periods and calculated using a 95<sup>th</sup> percentile regression on the assumed linear relationship between ET and GPP x VPD<sup>0.5</sup>. This relationship relies on stomatal optimality assumptions based on earlier work (Cowan & Farquhar, 1977; Farquhar & Sharkey, 1982; Zhou et al., 2014) which is also used to calculate the actual uWUE (uWUE<sub>a</sub>) with a regular linear regression. uWUE<sub>p</sub> is then related to T while the uWUE<sub>a</sub> is related to ET. uWUE<sub>p</sub> is estimated just once using all data available for the site while uWUE<sub>a</sub> is estimated over the time period during which T/ET is being predicted.

$$uWUE_a = \frac{GPP * VPD^{0.5}}{ET}, \tag{1}$$

$$uWUE_p = \frac{GPP * VPD^{0.5}}{T}, \tag{2}$$

160 Subsequently, T/ET is estimated using the ratio of potential to actual uWUE:



$$\frac{T}{ET} = \frac{uWUE_a}{uWUE_p}, \quad (3)$$

The uWUE assumptions make this method widely accessible to any flux site since only half-hourly flux data of GPP, VPD, and ET are needed in order to estimate T/ET from daily to annual timescales. However, the heavy reliance on GPP estimates from EC measurements mean that any uncertainties in GPP are amplified when predicting T using this method and the assumption of a constant uWUE<sub>p</sub> is violated at sites with a wide variety of vegetation types (Hu & Lei, 2021; Nelson et al., 2020; Reich et al., 2024; Stoy et al., 2019; Zhou et al., 2016). Additionally, the assumption that T=ET does not hold true throughout the day in ecosystems with sparse vegetation or where evaporation is never negligible such as in wetland ecosystems (Eichelmann et al., 2022; Li et al., 2019; Reich et al., 2024; Zhou et al., 2016). Interception evaporation is also ignored in this method as days with and immediately following rainfall are filtered out before the partitioning begins.

Berkelhammer et al. (2016) follows a similar procedure with similar assumptions (BH16), however, after plotting ET against GPP x VPD<sup>0.5</sup>, the GPP values are binned, and the minimum ET value is found for each bin. These minimum ET values are then thought to represent times when T/ET = 1 and the rest of the ET values are used to estimate T:

$$\frac{T}{ET} = \frac{\min_{GPP} \|ET\|}{ET_{flux}}, \quad (4)$$

However, because this method keeps the assumption from the ZH16 method whereby T/ET approaches 1 at sub-daily timescales, the same limitations apply with regards to application to ecosystems where E consistently and significantly contributes to ET. Additionally, assuming there is a linear relationship between ET and GPP x VPD<sup>0.5</sup> assumes a constant direct response of stomatal conductance to VPD which is not met under low VPD conditions (Addington et al., 2004; Day, 2000; Ocheltree et al., 2014). However, rainy days are not filtered out from the dataset, so while interception evaporation is not directly estimated, it is included in E estimates.

### 3.1.2 Stomatal conductance

Li et al. (2019) partitions ET using previously established assumptions of canopy and aerodynamic resistances (Monteith, 1965; Penman, 1948; Shuttleworth and Wallace, 1985). This method (LI19) estimates ecosystem conductances to sidestep the assumption that T/ET approaches 1. Here, a parameter optimization is added to an ecosystem conductance ( $G_s$ ) model (Lin et al., 2018) to separate surface conductances. This method excludes rainy periods and times when canopy interception contributes to ET so that  $G_s$  can be split into soil ( $G_{soil}$ ) and canopy ( $G_{veg}$ ) conductances, or soil evaporation and canopy transpiration, respectively, and  $G_s$  is calculated using EC data in the inverted Penman-Monteith equation using:

$$G_s = G_{soil} + G_{veg} = G_0 + G_1 \frac{GPP}{VPD_1^m}, \quad (5)$$



190  $G_s$  and GPP values are binned according to soil moisture, and a non-linear regression is run on Equation 5 to fit the ecosystem-level parameters:  $G_0$ ,  $G_1$ , and  $m$ .  $G_{soil}$  and  $G_{veg}$  can then be calculated in each soil moisture bin and ET is partitioned using assumptions similar to Shuttleworth & Wallace (1985):

$$\frac{T}{ET} = \frac{G_{veg}}{G_s}, \quad (6)$$

$$\frac{E}{ET} = \frac{G_{soil}}{G_s}, \quad (7)$$

195 Parameterizing  $m$  allows VPD's dependence on GPP to vary depending on vegetation type, a strength compared to methods using the assumption from Zhou et al. (2014) where a constant  $m$  of 0.5 assumes an optimal linear relationship between ET and GPP  $\times$  VPD<sup>0.5</sup> regardless of ecosystem type. However, LI19 was founded on the assumption that  $G_s$  is the sum of soil and canopy conductances, which is only true assuming there is a constant temperature throughout the canopy and soil surface, and not held in heterogeneous ecosystems (Li et al., 2019). Additionally, the exclusion of all rainy data has greater limitations in wet ecosystems where canopy interception is rarely negligible, and the necessity of soil moisture data limits its applicability to all flux sites (Hu and Lei, 2021; Li et al., 2019).

200 Perez-Priego et al. (2018) also partitions ET using model predicted ecosystem conductances (PP18). Starting with the assumption of optimality theory on a big-leaf canopy, the patterns of canopy-scale internal leaf-to-ambient CO<sub>2</sub> ( $\chi$ ) are modelled based on temperature, elevation, and VPD. Optimality theory ensures that the model parameters are estimated assuming the big-leaf canopy model minimizes  $T$  while maximizing photosynthesis. Then using GPP in conjunction with  $\chi$ , as well as the ambient CO<sub>2</sub> mixing ratio and molar air density, ecosystem stomatal conductance ( $g_c$ ) is modelled.  $T$  is then estimated by:

$$T = 1.6 \cdot g_c \cdot VPD, \quad (8)$$

210 Where 1.6 is the diffusivity factor for CO<sub>2</sub> and water vapor. PP18 avoids the assumption that ecosystem ET equals  $T$  however, upon application of PP18, Nelson et al. (2020) found that the model was not always able to converge to realistic  $T$  values, with 30% of predictions being unusable. The method also relies on GPP estimates and therefore is impacted by the uncertainties and biases of those values (Eichelmann et al., 2022; Nelson et al., 2020; Zhou et al., 2016). Additionally, to optimize the PP18 model, rainy periods and times with interception evaporation must be ignored which may lead to an overestimation of WUE and in turn underestimation of  $T$  (Perez-Priego et al., 2018).

### 3.1.3 Machine learning methods

215 More recently, several approaches using machine learning have been established to partition ET. Nelson et al. (2018) introduced the Transpiration Estimation Algorithm (TEA18) which uses a Random Forest regressor (Breiman, 2001) and isolates periods when  $T/ET \approx 1$  to estimate ecosystem WUE. The model achieves this by calculating the conservative surface wetness index to determine periods likely to have wet surfaces and excluding them from the training dataset. In order to account



for further instances of E in the training dataset, a 75<sup>th</sup> percentile of ecosystem WUE is then used as the model output. This predicted WUE ( $WUE_{pred}$ ) can then be used to calculate T on half hourly intervals:

$$220 \quad T = \frac{GPP}{WUE_{pred}}, \quad (9)$$

TEA18 can be easily applied to EC sites as it only requires GPP, ET, and simple meteorological data as inputs. However, because the model trains on dry periods where it is assumed that T/ET approaches 1, the behavior of WUE on rainy days and periods with interception evaporation will not be well represented in the model output. This leads to an overestimation of E in the training dataset and subsequent underestimation of T for ecosystems with sparse vegetation and wetland sites (Hu and Lei, 225 2021; Nelson et al., 2018; Reich et al., 2024).

Alternatively, Eichelmann et al. (2022) established a partitioning method (EE22) using an artificial neural network (Bishop, 1995) that assumes negligible nighttime transpiration values so therefore:

$$ET_{night} \approx E, \quad (10)$$

Daytime E is then predicted using measured nighttime ET values, similar to established methods of partitioning NEE into GPP and respiration based on nighttime NEE values (Reichstein et al., 2005). Because there are no underlying assumptions that T/ET approaches 1, it is easier to apply this method to ecosystems with large contributions of E. By focusing on nighttime E, the model training process accounts for nocturnal interception evaporation but may fail to properly constrain daytime interception evaporation in E estimates. This is one of the few partitioning approaches that does not rely on any assumptions of the relationship between CO<sub>2</sub> uptake and water loss through stomata, making it a stronger method for wetlands and other 235 ecosystems where E is never negligible and circumventing the need for GPP values.

However, while avoiding the assumption of zero E values, this method defaults to an assumption of zero T values, which is not met in every ecosystem and must be verified at sites before implementation (Dawson et al., 2007; Di et al., 2019; López et al., 2021a; Siddiq & Cao, 2018; Wang et al., 2021; Zeppel et al., 2010). EE22 also requires domain knowledge of the site for model feature selection, although this has been adjusted by Stapleton et al. (2022) who introduced a machine learning 240 framework consisting of 8 algorithms to identify the highest performing model for ET partitioning. The framework uses the assumptions from EE22 to estimate daytime E from nighttime ET measurements but conducts recursive feature elimination before training the model, a more objective approach as opposed to manual feature selection.

### 3.1.4 High frequency data

Using high-frequency data, Scanlon & Kustas, 2010 (SK10) established a method using the assumptions of flux variance 245 similarity (FVS; Scanlon & Kustas, 2010; Scanlon & Sahu, 2008). This method is based on the Monin-Obukhov similarity theory assuming that both stomatal and non-stomatal components of carbon (c) and water (q) fluxes independently adhere to FVS. The stomatal processes, both photosynthesis and transpiration are thought to have a q-c correlation of -1, with the non-stomatal process of respiration and evaporation degrading this perfect correlation. Scanlon and Sahu (2008) introduced the



idea that the degree of this degradation can be used to infer the magnitude of the non-stomatal processes. Leaf-level WUE is  
250 the only additional information needed to establish the relationship between the stomatal and non-stomatal processes in the  
carbon flux and estimate the components of both  $q$  and  $c$ . However, if leaf-level measurements are not available, WUE can be  
estimated from flux measurements and the ratio of molecular diffusivities for carbon dioxide and water vapor.

Because large-scale eddies can affect the assumptions on which the FVS theory is based, wavelet filtering is required  
to remove the low-frequency data from the time series. This introduces a complication in the application of the method as this  
255 filtering requires high-frequency data which is not often publicly available or easily accessible. Additionally, SK10 is  
computationally heavy as it uses optimization to solve the correlation between photosynthesis and respiration as well as the  
variance of photosynthesis. Fortunately, Skaggs et al. (2018) building on Palatella et al. (2014), solved these two parameters  
using algebra, significantly reducing computational time. Skaggs et al. also established Fluxpart, a free, open-source Python 3  
module that runs the SK10 partitioning method on high frequency data. Fluxpart makes SK10 significantly more accessible to  
260 researchers and subsequently increased the use of this partitioning method. However, the need for high-frequency datasets  
remains the largest obstacle for widescale application of SK10. Additionally, the assumption that WUE remains constant over  
a given time interval is not representative of sites with significant heterogeneous vegetation or in ecosystems with a well-  
developed understory (Eichelmann et al., 2022; Scanlon & Kustas, 2010; Zhou et al., 2016). The default leaf-level WUE  
estimation used in Fluxpart is:

$$265 \quad WUE = \frac{\frac{1}{1.6} * (c_a - c_i)}{q_a - q_i}, \quad (11)$$

Where  $c_a$  ( $q_a$ ) and  $c_i$  ( $q_i$ ) are the ambient and intercellular concentrations of  $\text{CO}_2$  ( $\text{H}_2\text{O}$ ), respectively and 1.6 is the diffusivity  
factor for  $\text{CO}_2$  and water vapor. There are several parametrization schemes to estimate  $c_i$ . Commonly, these assumptions are  
made:  $c_i$  is a constant value,  $c_i/c_a$  is a constant ratio, or  $c_i/c_a$  has a linear or square root relationship with VPD (Campbell and  
Norman, 1998; Katul et al., 2009; Kim et al., 2006; Morison and Gifford, 1983; Sinclair et al., 1984). Alternatively, WUE can  
270 be optimized using assumptions of the relationship between  $c$ ,  $q$ , and VPD (Scanlon et al., 2019).

Like SK10, the Modified Relaxed Eddy Accumulation method (TH08) introduced by Thomas et al. (2008) built on  
earlier work by Businger & Oncley (1990) to assume that the turbulent transport of non-stomatal components of carbon and  
water fluxes are similar. This method uses multi-scalar octant analysis to identify conditions where the  $q$  and  $c$  fluxes are equal  
to the soil flux component, or evaporation. The first octant (O1) is defined when the vertical velocity ( $w'$ ),  $c'$ , and  $q'$  are all  
275 greater than 0 (where  $w'$ ,  $c'$ ,  $q'$  are fluctuations from concurrent measurements), and using data that fits these criteria,  
evaporation is estimated as:

$$E_{TH08} = \beta \sigma_w \frac{\sum_{i=1}^N I_H q'_i}{\sum_{i=1}^N I_{H,w+}_i}, \quad (12)$$

Where  $N$  is the number of samples in the time series,  $\beta$  is the ratio between the standard deviation of the vertical velocity ( $\sigma_w$ )  
and the mean vertical velocities in updrafts and downdrafts, and  $I_H$  and  $I_{H,w+}$  are hyperbolic thresholds. Because O1 is defined



280 when  $w' > 0$ , the TH08 method only accounts for updrafts, an approach later modified to include downdrafts in the Conditional Eddy Accumulation method (TH08b; Zahn et al., 2024). Another expansion of TH08 was introduced when Zahn et al. (2022) created the Conditional Eddy Covariance method (ZN22) by stating that conditions within O1 were not equal to soil evaporation but were instead proportional. They then define a second octant (O2) for when  $w'$  and  $q'$  are greater than 0 and  $c'$  is less than 0 to represent transpiration conditions. Then conditional covariances can be computed for E and T:

$$285 \quad f_E = \frac{1}{N} \sum I_E w' q' \quad , \quad (13)$$

$$f_T = \frac{1}{N} \sum I_T w' q' \quad , \quad (14)$$

Where  $I_E$  and  $I_T$  are indicator functions equal to either 1 or 0 depending on if the data falls within O1 or O2. Because of the assumption that  $f_E$  and  $f_T$  are representative of the stomatal and non-stomatal fluxes, the ratio of  $f_E$  to  $f_T$  is then equal to the ratio of E to T. This approach was later modified to include WUE, if known, to help further constrain the carbon flux (ZN22b; Zahn et al., 2024). However, due to the need for high frequency datasets and the high computational time both TH08 and ZN22 require, they are difficult to apply to flux sites and infrequently chosen as the preferred ET partitioning method. Another limitation of all high frequency-based methods (SK10, TH08, and ZN22) is that because they distinguish stomatal and non-stomatal sources of water vapor based on the  $q$ - $c$  correlation, interception evaporation from the canopy surface can be incorrectly represented in the transpiration estimates (Ranjbar et al., 2026; Shih et al., 2025; Zahn et al., 2022).

### 295 **3.1.5 Linear regression**

The method introduced by Scott & Biederman (2017) (SB17) uses linear regression on multiyear datasets to derive a direct relationship between measured annual ET and gross ecosystem photosynthesis (GEP where  $GEP = -GPP$ ) where the x-intercept represents an average E estimate when  $GEP = 0$ . Then by inverting the regression whereby GEP serves as a predictor of ET, they define the slope of the regression as the marginal ecosystem WUE ( $WUE_{mar}$ ), which is then used to calculate T by:

$$300 \quad T = mxGEP, \quad (15)$$

Where  $m$  is the inverse of  $WUE_{mar}$  ( $WUE_{mar}^{-1} = \Delta ET / \Delta GEP$ ) and  $x$  is the ratio between the inverse of transpirational WUE ( $T/GEP$ ) and  $WUE_{mar}^{-1}$ . Because the regression is defined from periods without transpiration, interception evaporation is accounted for in E estimates. There is also no need for the assumption  $T/ET$  approaches 1 in SB17, unlike with the uWUE methods, because potential WUE, or  $WUE_{mar}$ , is calculated on an average monthly basis by comparing multiple years of data. This makes SB17 more applicable to water-limited and wetland sites, however, the site must display consistent ecological response progressions between years in order for the monthly estimate of  $WUE_{mar}$  to accurately represent the ecosystem (Eichelmann et al., 2022; Hu and Lei, 2021; Reich et al., 2024; Scott and Biederman, 2017).

While this method is more accessible as it does not require high frequency data or a priori plant WUE information, it does require a minimum of 3 years of data, with ideal data sets of 5-7 years in length in order to produce significant results



310 (Eichelmann et al., 2022; Li et al., 2019; Scott and Biederman, 2017). This method also relies on the assumption of a strong relationship between yearly ET and GPP, which is not valid in ecosystems with high water availability (Hu and Lei, 2021; Scott and Biederman, 2017).

Because of the aggregation of data over years, SB17 inherently suppresses the influence of rainy periods, making it unsuitable for dryland ecosystems where an influx of precipitation causes substantial changes in ecosystem processes (Reich et al., 2024). A variation of SB17 was introduced by Reich et al. (2024) who created a semi-mechanistic model in a Bayesian framework called the Dynamic Evapotranspiration Partitioning Approach for Rapid Timescales (SB17b). SB17b operates similarly to SB17 but at a finer temporal scale and estimates weekly WUE by constraining abiotic evaporation and calculating ET and T on daily timescales:

$$ET_{daily} = m_{w(d)}GPP_d + E'_d, \quad (16)$$

320  $ET_{daily} = m_{w(d)}GPP_d + E'_d, \quad (17)$

Where  $E'_d$  is the intercept of the regression (i.e. value of ET when GPP = 0),  $m_{w(d)}$  is the inverse of weekly WUE, and  $GPP_d$  is daily GPP. While SB17 assumed that E is invariant across years of data for an individual month, SB17b allows E to vary on daily timescales, introducing the influence of rainy periods on T, E, and WUE, and like SB17, interception evaporation is included in E estimates. However, the model uses process-based equations to parameterize abiotic evaporation where the equations do not account for vegetation cover and therefore are unable to represent the full heterogeneity of a tower's footprint (Reich et al., 2024).

### 3.2 Geographic and climatic distribution of studies applying reviewed ET partitioning methods

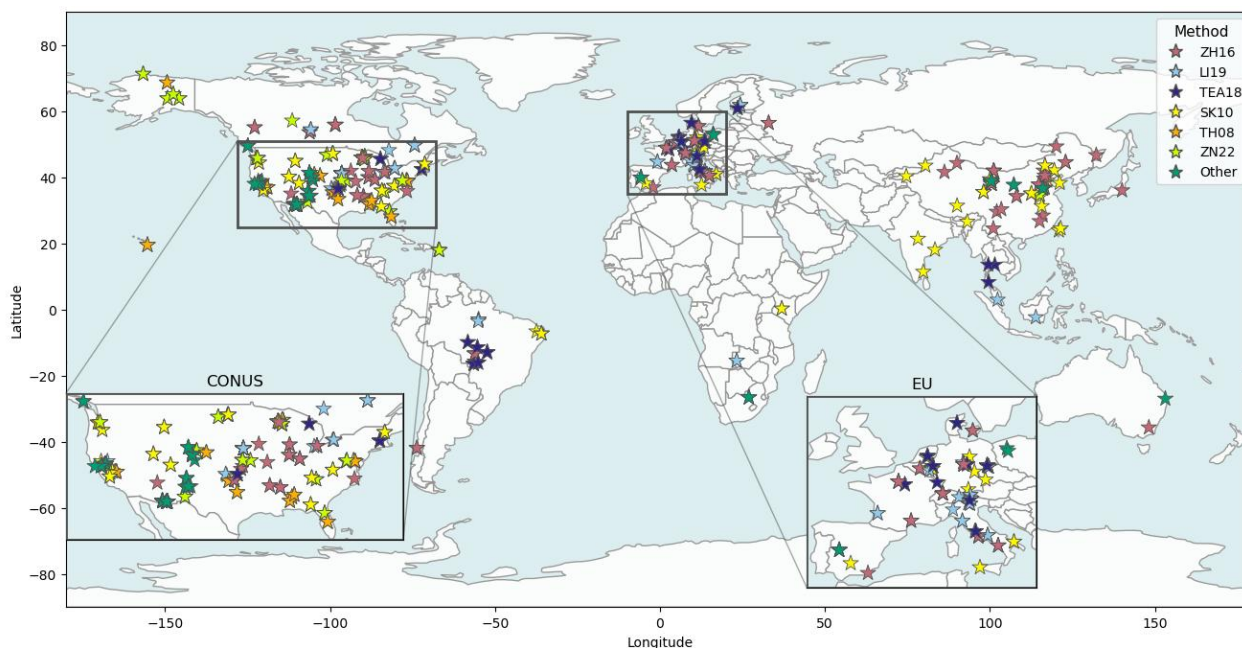
Tables summarizing published studies (site location, biome, T/ET results, and comparisons to other methods) using six of the most widely tested EC-based partitioning methods (ZH16, LI19, PP18, TEA18, SK10, SB17) are shown in the appendix (Tables A1-A6), including a table for methods with limited testing ( $N_s \leq 5$ ) (Table A7). If a study used more than one partitioning method, it was repeated in each applicable table with a note as to how the results compared between the methods. In instances where studies applied a partitioning method but did not give results including T/ET, T, E, and/or ET quantities, a qualitative summary of important findings was included as well. As there were limited studies presenting paired results from two or more partitioning methods on the same dataset, the following comparison refers to average ecosystem type results and is not representative of how method estimates compare directly unless otherwise stated.

Table 2: Mean and standard deviation of transpiration to evapotranspiration ratios (T/ET) calculated in published studies using EC-based ET partitioning methods (only methods with total  $N_R > 5$  are shown). Quantitative results of annual and growing season means reported in Tables A1-A6 were used for calculating the average (Avg) and standard deviation (STD). For croplands (CRO), if two or more crops were reported on in the same study, they were each represented as an individual record.



Studies reporting on several biomes without distinction were represented in Misc. The plant functional types (PFT) of the ecosystems were identified with GRA: grassland, DBF: deciduous broadleaf forest, ENF: evergreen needleleaf forest, EBF: evergreen broadleaf forest, MF: mixed forest, SAV: savanna, WSA: woody savanna, OSH: shrubland, BSV: bare sparse vegetation, WET: wetland.  $N_R$ : number of records identified, uWUE: underlying water use efficiency. Method abbreviations: 345 ZH16: Zhou et al. (2016), LI19: Li et al. (2019), PP18: Perez-Preigo et al. (2018), TEA18: Nelson et al. (2018), SK10: Scanlon & Kustas (2010), SB17: Scott & Biederman (2017).

Method type	Method	T/ET	GRA	EBF	CRO	ENF	MF	WET	DBF	SAV	OSH	WSA	BSV	Misc.
uWUE	ZH16	$N_R$	15	1	28	7	3	1	7	2	4	2	1	4
		Avg.	0.54	0.52	0.51	0.49	0.49	0.49	0.49	0.48	0.42	0.42	0.37	0.49
		(STD)	(0.10)		(0.11)	(0.05)	(0.10)		(0.05)	(0.13)	(0.16)	(0.04)		(0.08)
Stomatal conductance	LI19	$N_R$	2	1	3	1	0	1	2	0	0	1	0	2
		Avg.	0.67	0.54	0.55	0.75	-	0.56	0.58	-	-	0.61	-	0.70
		(STD)	(0.16)		(0.10)				(0.31)					(0.05)
	PP18	$N_R$	0	0	2	1	0	2	0	0	0	1	0	1
		Avg.	-	-	0.66	0.55	-	0.29	-	-	-	0.60	-	0.45
		(STD)			(0.28)			(0.08)						
Machine learning	TEA18	$N_R$	4	1	11	3	1	0	6	3	2	2	0	3
		Avg.	0.64	0.78	0.70	0.68	0.51	-	0.71	0.69	0.47	0.69	-	0.67
		(STD)	(0.12)		(0.14)	(0.60)			(0.06)	(0.08)	(0.18)	(0.03)		(0.09)
High frequency	SK10	$N_R$	3	0	18	1	0	1	3	0	0	0	0	1
		Avg.	0.56	-	0.67	0.53	-	0.46	0.73	-	-	-	-	0.52
		(STD)	(0.20)		(0.09)				(0.17)					
Linear regression	SB17	$N_R$	2	0	2	0	0	0	1	2	2	0	0	0
		Avg.	0.59	-	0.67	-	-	-	0.40	0.68	0.47	-	-	-
		(STD)	(0.11)		(0.04)					(0.09)	(0.04)			



350 **Figure 2: Geographical locations of data records found in literature search.** Method types: underlying water use efficiency: ZH16, stomatal conductance: LI19, machine learning: TEA18, high frequency: SK10, TH08, ZN22. “Other”  
 comprised the following method types: underlying water use efficiency: BH16, stomatal conductance: PP18, machine learning:  
 EE22, linear regression: SB17 and SB17b. Global studies featuring more than 50 sites across 4 continents are not featured on  
 the map. CONUS: continental United States, EU: Europe, ZH16: Zhou et al. (2016), LI19: Li et al. (2019), PP18: Perez-Preigo  
 355 et al. (2018), TEA18: Nelson et al. (2018), SK10: Scanlon & Kustas (2010), SB17: Scott & Biederman (2017), BH16:  
 Berkelhammer et al. (2016), EE22: Eichelmann et al. (2022), TH08: Thomas et al. (2008), ZN22: Zahn et al. (2022), SB17b:  
 Reich et al. (2024).

ZH16 has been studied in all major biome types across all continents (excluding Antarctica) across 53 studies (Tables 2, A1;  
 360 Fig. 2). The majority of reported results ( $N_R$ ) were in croplands (30) representing a variety of annual and perennial crops (e.g.  
 soybeans, rice, cotton, wheat, maize, etc.). Grasslands (22) and forests (32 across all forest types) were also frequently reported  
 on. ZH16 was applied the most in Asian (30) and North American (18) sites (Fig. 2). SK10 usage was reported in 40 studies,  
 mostly in croplands (29) with an emphasis in wheat (8), maize (6), and various orchards (6). SK10 was also heavily tested  
 across different forest types (11) and was applied the most in North America (20) however several continents and biomes were  
 365 not tested (Tables 2, A5; Fig. 2). TEA18 was the next most tested method, appearing in 21 studies (Table A4). Like SK10 and  
 ZH16, TEA18 was tested the most in forests (16) and croplands (12) and across Asia (8) and North America (7; Fig 2).

The remaining methods had a considerable drop in number of studies with the next highest tested method being SB17  
 featured in 7 papers where 6 were in North America (Table A6; Fig. 2). PP18 and LI19 were each used in 6 and 7 studies,



respectively, however both methods were included in global studies (Tables A2, A3; Maes et al., 2020; Nelson et al., 2020).  
370 The BH16 method was used in 5 studies, predominately in North America (3; Table A7, Fig. 2), 3 of which were in evergreen  
forests (mean = 0.66). The high frequency methods from ZN22 and TH08 were used in 5 and 3 identified studies, respectively  
(Table A7) and while they often agreed with each other, both tended to be higher than SK10 estimates. EE22 has been applied  
in 3 studies, 2 in North America and 1 in Asia (Table A7, Fig. 2). SB17b was only applied once in North America, and a  
combined method of ZH16 and SB17 was used once in a GRA / WSA ecosystem in North America (Table A7; Yuan et al.,  
375 2021).

### 3.3 Comparison of ET partitioning method results from identified studies

ZH16 consistently produced the lowest T/ET values when compared to other EC-based partitioning methods (Figs. 3, 4). In  
fact, PP18 was the only method to predict lower T values than ZH16, particularly in wetlands (Tables 2, A1, A3; Fig. 3).  
However, PP18 was only used in 6 studies so it is yet undetermined whether the low estimations were a systemic issue with  
380 the method or only apparent in specific ecosystems (Table A3, Fig 3). On the other hand, TEA18 estimates consistently had  
either the highest or comparable T/ET value estimates when directly compared to other EC-based methods in 14 of 14 studies  
(Table A4, Figs. 3, 4). These high estimates agreed well with many non-EC based partitioning methods (i.e., sap flow, two-  
stage theory of bare soil evaporation, TSEB-SM, and LSMs). TEA18 estimates, while slightly higher, were also similar in  
magnitude to SK10 estimates, although the high frequency-based method has overwhelmingly been tested in crop systems  
385 with limited testing in other ecosystems (Fig. 3; Table A5). The other high frequency-based methods (TH08 and ZN22) showed  
similar results to SK10 with TH08 typically producing higher T/ET estimates than SK10 and ZN22, however, their full range  
of abilities cannot yet be quantified as they have only been tested in 5 studies collectively (Table A7). The linear regression-  
based methods also had limited testing, with SB17 being used in 6 studies and SB17b in only 1, however this may be due to  
the hefty requirement of ideal datasets having 5-7 years of data (Tables A6, A7). SB17 produced similar T/ET trends as other  
390 methods but with lower values when directly compared to TEA18, EE22 and SB17b, and higher values when directly compared  
to ZH16 and LI19 (Table A6). SB17b was only found to have been tested in one study where it estimated very high T/ET  
values across 5 ecosystem types (Reich et al., 2024). However, it is hard to determine if this method systematically produces  
high T estimates due to its assumption of homogenous vegetation, or if the high average T estimates are due to a small sample  
size (Table A7). LI19, a stomatal conductance-based method, estimated higher or similar values to ZH16, with lower values  
395 than SB17 and TEA18 (Table A2). The BH16 method was only used in 5 studies and did not show any consistency in the  
magnitude of its T/ET estimates compared to other methods. In fact, in one study it estimated lower values than ZH16 (Räsänen  
et al., 2022), but in other studies showed similar or higher estimates than sap flow-based and TSEB methods (Cammalleri et  
al., 2024; Dukat et al., 2023), two independent methods shown to previously agree well with high estimates from TEA18.

When summarizing T/ET estimates on a global scale, four studies presented a mean annual T/ET estimate across at least  
400 four biomes using at least 50 sites. ZH16 presented an average global annual T/ET of 0.52 ( $N_S=3$ ; Cao et al., 2022; Nelson et  
al., 2020; Xue et al., 2023), TEA18 with 0.69 ( $N_S=2$ ; Nelson et al., 2020; Xue et al., 2023), PP18 with 0.45 ( $N_S=1$ ; Nelson et



al., 2020), and LI19 with 0.66 ( $N_S=1$ ; Maes et al., 2020). Even with this limited range of testing, the global averages still show low estimates from ZH16 and PP18 with moderate estimates from LI19 and the highest T/ET estimates from TEA18. The global, annual mean of T/ET across the 4 methods in 4 studies was  $0.577 \pm 0.04$  (Fig. 3). This is comparable to the average T/ET value ( $0.584 \pm 0.01$ ) found from all records regardless of partitioning method or ecosystem (Fig. 3).

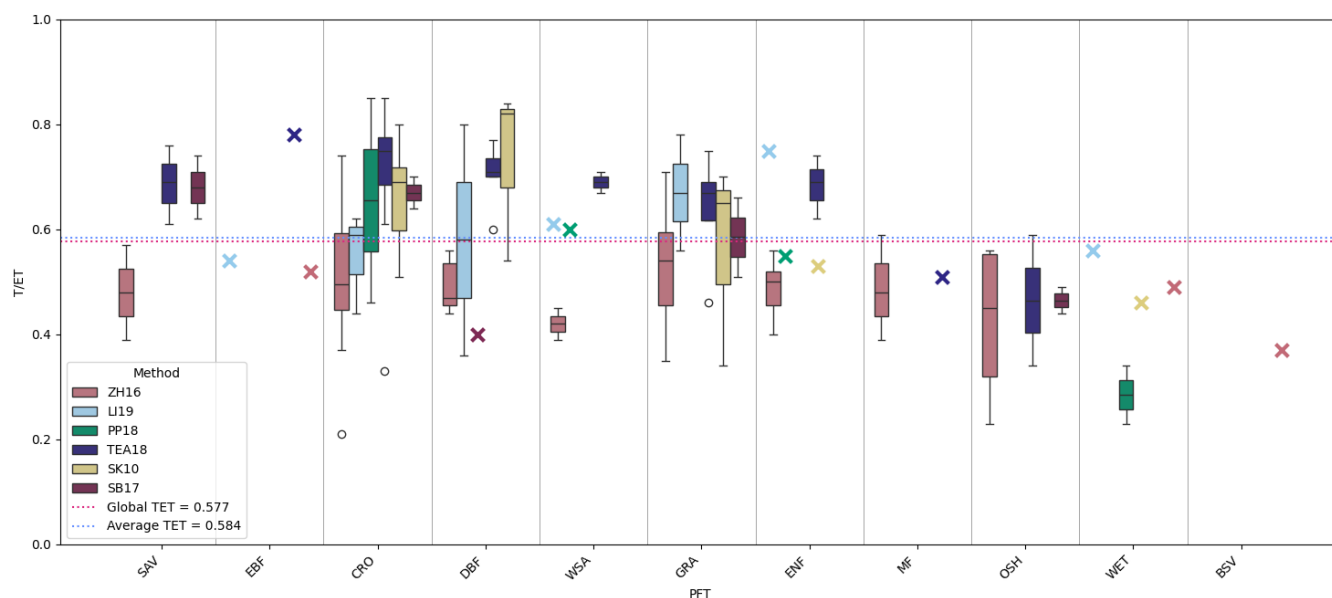


**Figure 3: Box and whisker plots of ET partitioning methods estimates across plant functional types (PFT) from all quantitative data extracted from the literature search.** Method and PFT combinations with only 1 record are shown as an X. Only methods with more than 5 records are included. PFTs are ordered by decreasing average T/ET estimates across records. The red dotted line is the global T/ET value estimated from studies that included multiple ecosystem types across more than 50 sites. The average T/ET value represents all records from all studies and is shown in the blue dotted line. Methods: ZH16: Zhou et al. (2016), LI19: Li et al. (2019), PP18: Perez-Preigo et al. (2018), TEA18: Nelson et al. (2018), SK10: Scanlon & Kustas (2010), SB17: Scott & Biederman (2017). SAV: savanna, EBF: evergreen broadleaf forest, WSA: woody savanna, CRO: cropland, DBF: deciduous broadleaf forest, ENF: evergreen needleleaf forest, GRA: grassland, MF: mixed forest, OSH: open shrubland, WET: wetland, BSV: bare sparse vegetation.

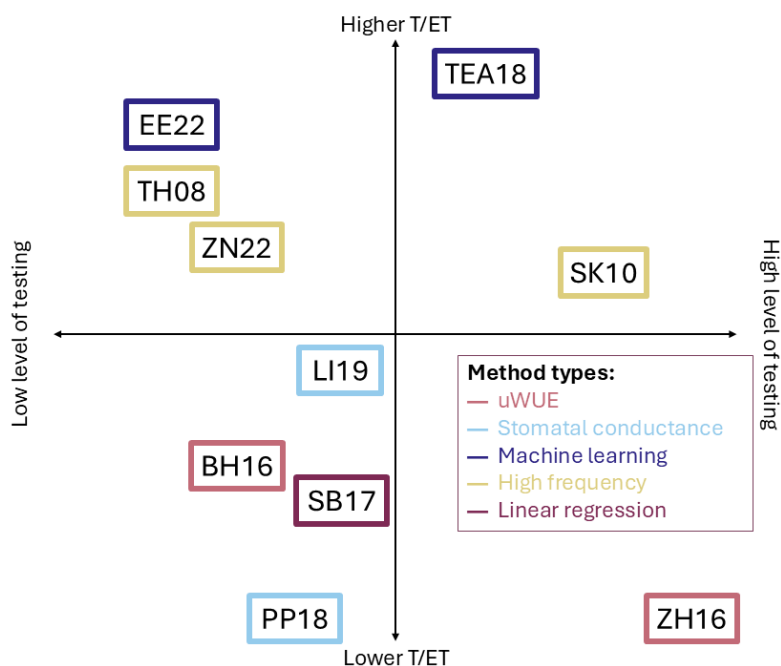


**Figure 4: Summarized results of relative T/ET output from the 10 independent methods identified in this review and their level of testing.** Methods were placed on the x-axis according to number of studies with methods left of the origin

420 appearing in less than 10 studies. Y-axis placement was determined by relative T/ET estimates compared across all studies featuring two or more identified methods. Methods: ZH16: Zhou et al. (2016), BH16: Berkelhammer et al. (2016), LI19: Li et al. (2019), PP18: Perez-Preigo et al. (2018), TEA18: Nelson et al. (2018), EE22: Eichelmann et al. (2022), SK10: Scanlon & Kustas (2010), TH08: Thomas et al. (2008), ZN22: Zahn et al. (2022), SB17: Scott & Biederman (2017). uWUE: underlying water use efficiency.

### 425 3.3.1 Regional drivers of T/ET

LAI and similar vegetation indices were found to be the most common identified driver of T/ET in the studies included in this review (Li et al., 2024d; Lowry et al., 2021; Restrepo-Coupe et al., 2023; Sun et al., 2020; Wagle et al., 2020; Wang et al., 2016; Zahn et al., 2022; Zhou et al., 2016). While LAI influenced T/ET dynamics within a site/ecosystem, a higher LAI did not always indicate higher transpiration rates across sites/ecosystems, as the highest T values were found in SAV ecosystems and relatively low T was estimated for MF (Fig. S1). SWC, especially during dry conditions, was also found to be one of the most important drivers of T/ET in several studies across global biomes (da Rocha et al., 2022; Liu et al., 2022b; Nie et al., 2021). A tall grass prairie study found that T/ET was strongly positively correlated with sub surface SWC and slightly negatively correlated with upper layer SWC, agreeing with results from GRA and DBF studies (da Rocha et al., 2022; Deb Burman et al., 2022; Scott et al., 2021; Xu et al., 2021). Air temperature and VPD were also found to have significant impacts



435 on T/ET values and trends across studies (da Rocha et al., 2022; Eichelmann et al., 2022; Nie et al., 2021; Sun et al., 2020; Xu  
et al., 2021). Across biomes, transpiration ratios were found to be the highest in savannas and evergreen broadleaf forests while  
the lowest ratios occurred in wetlands and deserts (Fig. S1).

## 4 Discussion

### 4.1 Identified partitioning methods and common uncertainties

440 The systematic literature on EC-based methods identified 10 independent ET partitioning methods that have been applied  
across 123 studies with testing spanning 11 plant functional types. Two methods based on the concept of uWUE (ZH16 and  
BH16) predicted low estimates of T/ET across all ecosystems while machine learning methods (TEA18 and EE22) consistently  
estimated higher values when compared to other methods (Figs. 3, 4). The magnitude discrepancy between EC-based methods,  
particularly between ZH16 and TEA18, may be due to the assumption that WUE is optimized at the leaf-level, however, this  
445 assumption has a weak theoretical basis (Nelson et al., 2020). ZH16 estimated WUE using a 95<sup>th</sup> percentile threshold on the  
relationship between GPP x VPD<sup>0.5</sup> and ET while TEA18 used the 75<sup>th</sup> percentile. The upper values in the 95<sup>th</sup> percentile may  
have led to an overestimation of WUE and subsequent underestimation of T, a systematic problem seen in the BH16 method  
as well (Ma et al., 2020; Nelson et al., 2020).

Comparing the limitations of the partitioning methods, perhaps the most prevalent is the use of GPP in T estimates. GPP  
450 is itself, a modelled value as EC cannot directly measure GPP just as it cannot directly measure T. So, NEE partitioning  
methods are used to estimate GPP (Lasslop et al., 2010; Reichstein et al., 2005). However, this means that any uncertainties  
and biases in the modelled GPP are inherently linked to the subsequent modelled T. The methods that use binned GPP or GPP  
percentiles (i.e., ZH16, TEA18, LI19, and BH16) will be greatly affected by short-term errors of GPP if they introduce enough  
outliers to skew the regression. However, they will not be impacted by consistent, systematic GPP alterations as shown by the  
455 fact that T estimates were not affected when the nighttime and daytime NEE partitioning methods were applied (Nelson et al.,  
2020). PP18 on the other hand uses GPP to directly calculate ecosystem stomatal conductance which is then used to estimate  
T and therefore will be sensitive to both short-term and systematic GPP biases and errors. Additionally, the lack of agreement  
between GPP-based methods may indicate that the assumed optimal relationship between stomatal carbon gain and water loss  
is not maintained across diverse ecosystems and in fact, that the relationship varies by plant type and is changing with the  
460 warming climate (Hatfield and Dold, 2019; Medlyn et al., 2017; Nelson et al., 2020).

Another source of large uncertainties is the handling of interception evaporation between the methods. The stomatal  
conductance-based methods ignore this process completely even with studies reporting that 8.5-10% of annual rainfall is  
intercepted by plant surfaces globally with some regional estimates reaching up to 50% depending on ecosystem type (Fischer  
et al., 2026; Lian et al., 2022; Zhong et al., 2022). EE22 does not remove wet periods from the training data like TEA18,  
465 however it still neglects to account for daytime canopy interception rates that differ from their nocturnal counterparts



(Czikowsky & Fitzjarrald, 2009). In high frequency methods, the inattention to rainfall often results in interception evaporation being incorrectly partitioned into T which may be in part responsible for this method type's high T/ET estimates (Fig. 4).

#### 4.2 Global application of ET partitioning methods

ZH16, SK10, and TEA18 have been utilized to partition ET in many studies ( $N_S = 54, 40, \text{ and } 21$ , respectively) across even  
470 more datasets ( $N_R = 75, 57, \text{ and } 36$ , respectively). However, while 13 LI19 T/ET estimates have been reported across 6 studies,  
every other method has reported less than 10 studies. This limited range of experiments, especially rare instances where several  
methods have been applied to the same data record for comparison, emphasizes the need for further testing of all methods  
across all PFTs in order to pair T/ET estimates, fully evaluate the performance of each method, and reliably track global T  
trends (Fig. S2).

475 However, while direct comparisons of method estimations at specific EC sites are limited, there were still 4 identified  
studies that presented global T/ET values (Cao et al., 2022; Maes et al., 2020; Nelson et al., 2020; Xue et al., 2023). From  
these 4 studies presenting 7 estimates, an average annual T/ET value of  $0.577 \pm 0.04$  was determined (Fig. 3). This value was  
comparable to the average T/ET value calculated from every identified record in the literature search ( $T/ET = 0.584 \pm 0.01$ ;  
Fig. 3). While these averages were calculated independently, their correlation suggests an even representation of PFTs in  
480 accordance with their abundance were identified in the search.

The global values found in this study as well as the average T/ET value are consistent with a study using remote sensing  
data paired with an LSM and LAI measurements ( $0.57 \pm 0.07$ ; Wei et al., 2017), a satellite SIF based method ( $0.57 \pm 0.14$ ; Liu  
et al., 2022c), a hydrological LSM ( $0.59$ ; Wang-Erlandsson et al., 2014), and similar to a lateral flow based model ( $0.62 \pm$   
 $0.12$ ; Maxwell & Condon, 2016), the CMIP5 model ( $0.62 \pm 0.06$ ; Lian et al., 2018), and a previous synthesis study combining  
485 EC, sap-flow and isotopic partitioning methods ( $0.61 \pm 0.15$ ; Schlesinger & Jasechko, 2014). This study also falls within the  
bounds of an isotopic synthesis study ( $0.35\text{-}0.80$ ; Coenders-Gerrits et al., 2014) which adjusted previous uncertainty  
assumptions regarding isotopes where they reported a global T/ET range of  $0.80\text{-}0.90$  (Jasechko et al., 2013), and another  
synthesis using T, E, ET, with LAI data ( $0.38\text{-}0.77$ ; Wang et al., 2014). A mechanistic ecohydrological model, the remote  
sensing GLEAM model, the TSEB-SM, and satellite water vapor isotope measurements all found slightly higher global  
490 terrestrial T/ET values at  $0.70 \pm 0.09, 0.80, 0.73, \text{ and } 0.64 \pm 0.13$ , respectively (Fatichi and Pappas, 2017; Miralles et al., 2011;  
Paschalis et al., 2018; Xue et al., 2023).

#### 4.3 Transpiration trends and drivers

The dynamics of T/ET differed on diurnal, seasonal, and interannual timescales due to varying leaf area index (LAI), plant  
cover, and environmental conditions (Scott & Biederman, 2017). In regard to evolving global T trends, Xue et al. (2020) used  
495 ZH16 and found 12 of 67 flux sites had significant changes in T/ET over the past two decades seeing 5 sites with decreased  
T/ET and 7 sites with increased T/ET. They also found no consistent trends across biomes concerning LAI's influence on T/ET  
dynamics regardless of SWC. This juxtaposed many regionalized studies that repeatedly found LAI to be one of the most



important drivers for ecosystem T (Li et al., 2024d; Lowry et al., 2021; Restrepo-Coupe et al., 2023; Sun et al., 2020; Wagle et al., 2020; Wang et al., 2016a; Zahn et al., 2022; Zhou et al., 2016). The reliance on LAI is not only present in EC-based partitioning studies but also when using remote sensing based machine learning models, ecosystem resistance models, a method based on EC measurements with LSM data, and isotopic methods (Chen et al., 2024; Fatichi and Pappas, 2017; Gnanamoorthy et al., 2024; Good et al., 2014; Lu et al., 2023; Schlesinger and Jasechko, 2014; Wang et al., 2014). In fact, LAI and other similar vegetation indices can explain around 40% of annual variability in global T/ET (Wang et al., 2014; Wei et al., 2015). Significant impacts were seen on seasonal timescales as well where increased plant cover led to increased T/ET (Li et al., 2019; Scott and Biederman, 2017; Wang et al., 2010; Wei et al., 2015).

Another study found that the presence of drought increased global T/ET (Yang et al., 2025b) which is supported by findings of the influence of SWC on T in regional studies (da Rocha et al., 2022; Liu et al., 2022b; Nie et al., 2021; Wang et al., 2024a). Solar-induced chlorophyll fluorescence (SIF), VPD, and soil water content (SWC) have also been found to correlate with annual and seasonal T/ET dynamics on a global scale in various ecosystem models informed from remote sensing, sap flow, or LAI data (Li et al., 2024a; Pagán et al., 2019; Song et al., 2023a; Wei et al., 2017). However, even with known T/ET drivers, global estimates of T/ET still suffer from large uncertainties varying anywhere from 24-90% depending on the partitioning method used (Wei et al., 2017). More studies directly comparing several partitioning approaches on the same datasets are required to fully compare the methods so that a systematic framework for selecting an appropriate partitioning method can be established for future studies.

## 515 **5 Conclusions**

By conducting a comprehensive literature search for eddy covariance-based evapotranspiration partitioning methods, 10 independent methods were found to be tested across 123 studies. Two methods partition ET by assuming there is an optimal, linear relationship between ET and  $GPP \times VPD^{0.5}$ . Methods built from ecosystem conductance models also use the relationship between ET, GPP, and VPD, but there are no linear assumptions allowing the relationship to vary with vegetation type. For other methods using half-hourly EC data, two use machine learning to make T estimates from flux and meteorological data while one assumes a linear relationship between ET and gross ecosystem production. There were also 3 methods requiring high frequency EC data that assumed similar transport of non-stomatal and stomatal turbulent fluxes. All of the assumptions on which the various methods are based are ecosystem-dependent and no single method seems to be able to produce reliable T/ET estimates across all biomes. As such, method selection still must be guided by a priori site knowledge of vegetation characteristics, environmental conditions, and data availability.

Leaf area index was the most consistent driver of T/ET values and trends across studies with soil water content, VPD, and air temperature also playing significant roles depending on ecosystem type. From the identified studies, a global mean T/ET of 0.58 was calculated. This value is comparable to previous global studies using land surface models, remote sensing data, and isotopic partitioning approaches. This agreement lends confidence to the ability of eddy covariance-based methods



530 to capture ecosystem-scale ET partitioning even with common disadvantages among the methods such as the reliance on GPP estimates and the neglect of interception evaporation. However, while global studies, both eddy covariance-based and other, are converging on an annual T/ET estimate from terrestrial ecosystems, most T/ET estimates, regardless of their method of origin, remain largely unvalidated against ground truth measurements.

535 Currently, only 3 methods have been included in more than 10 studies and while North America, Europe, and Asia are well represented in the datasets, Africa and Oceania have been included in very few partitioning studies. Evergreen broadleaf forests and mixed forests also have limited testing; however, croplands and grasslands are well represented. Further testing of all methods, especially newly established methods and additional studies in underrepresented regions and ecosystem types will allow for better insights into how the methods assumptions hold in various ecosystems and will give more information into the changing trends and values of T and E under a warming climate.

## 540 6 Appendix A

### 6.1 ZH16

Table A1: Studies that have used the underlying water use efficiency partitioning method by Zhou et al. (2016) to calculate the transpiration to evapotranspiration ratio (T/ET). The timescales used in the T/ET calculations are listed as well as any comparisons to other ET partitioning methods. Locations are listed by FLUXNET site IDs when applicable, for any non-FLUXNET sites, the location is listed in accordance to how it was reported in the methods of each study. The plant functional types (PFT) of the ecosystems are identified with CRO: cropland, GRA: grassland, DBF: deciduous broadleaf forest, ENF: evergreen needleleaf forest, EBF: evergreen broadleaf forest, MF: mixed forest, SAV: savanna, WSA: woody savanna, OSH: shrubland, BSV: bare sparse vegetation, WET: wetland. GS: growing season, LAI: leaf area index, HRB: Heihe River Basin, TSEB: two source energy balance model, TSEB-SM: TSEB aided by soil moisture, LSM: land surface model. Methods: ZH16: Zhou et al. (2016), LI19: Li et al. (2019), PP18: Perez-Preigo et al. (2018), TEA18: Nelson et al. (2018), SK10: Scanlon & Kustas (2010), SB17: Scott & Biederman (2017).

Reference	PFT	Location	Calculation	T/ET	Notes
(Zhou et al., 2016)	CRO (corn)	US-Bo1, IB1, Ne1, Ne2, Ne3	Annual mean	0.69	
	CRO (soybean)	US-Bo1, IB1, Ne2, Ne3		0.62	
	GRA	US- Arb, Goo, Var, Wir		0.6	
	ENF	CA-NS3, NS5, US-NC2		0.56	
	DBF	US-Ha1, Moz, UMB, WCr		0.52	
(D'Acunha et al., 2024)	CRO (soybean)	Amazon agriculture, Cerrado agriculture Lucas do Rio Verde, Cerrado agriculture Jaciara	From annual T, ET totals	0.43	Lower T/ET estimates than with TEA18 method
	DBF			0.44	



	GRA WSA Misc.	Amazon forest Tanguro, Amazon forest Sinop, Pantanal forest Amazon pasture, Pantanal pasture Cerrado Campo sujo All Mato Grosso, Brazil sites (from above)	Annual mean	0.44 0.39 0.42	
(Liu et al., 2023)	CRO (rice)	Poyang Lake Basin, Jiangxi Province, China	GS mean	0.47	Lower T/ET estimates with direct seeded early rice vs. transplanted early rice
(Hu et al., 2018)	OSH DBF CRO (cotton) CRO (wheat/maize) GRA	HRB, Sidaoqiao HRB, Xitaizi HRB, Xinier HRB, Daman  HRB, Arou	Weekly mean	0.59 0.36 0.63 0.39  ~0.40	
(Nelson et al., 2020)	DBF GRA ENF Misc.	251 FLUXNET sites	Annual mean   Peak seasonal	0.45 0.43 0.40 0.52 0.58	Lower T/ET estimates than with TEA18 method, similar estimates to PP18
(Wang et al., 2020)	CRO (maize)	Yangling, Guanzhong Plain, China	GS mean	0.52	
(Peng et al., 2023)	CRO (wheat)	Yangling, Guanzhong Plain, China	GS mean	0.56	
(Hu & Lei, 2021)	CRO (wheat) CRO (maize)	Weishan, North China Plain	GS mean	0.52 0.46	Lower T/ET estimates but similar trends to the two-stage theory of bare soil evaporation, lower estimates than SB17, SK10, and TEA18
(Xu et al., 2021)	GRA ENF CRO (maize) BSV OSH MF	HRB, Arou HRB, Guantan HRB, Daman HRB, Huazhaizi HRB, Sidaoqiao HRB, mixed forest	Annual mean	0.53 0.52 0.59 0.37 0.56 0.59	
(Li et al., 2024d)	ENF	US-GLE	Annual mean	0.45	Decreased T/ET during bark beetle infestation that decreased LAI
(Han et al., 2018)	GRA	CN-NMG	GS mean	0.53	Decreased T/ET during prolonged drought period
(Gan and Liu, 2020)	CRO (maize) ENF GRA CRO (maize/wheat) CRO (orchard)	CN-YK, TYC CN-DYK, QYZ CN-TYG CN-DX  CN-MY	Annual mean	0.39 0.46 0.43 0.45  0.44	
(Paul-Limoges et al., 2022)	CRO (wheat) CRO (barley)	CH-Oe2 CH-Oe2	GS mean	0.48 0.37	Decreased diurnal and seasonal T/ET trends than TEA18 method
(Xu et al., 2024)	GRA	HRB, Arou	GS mean	0.54	T/ET values and trends follow SIB2 model (an LSM)



(Chen et al., 2023)	CRO (maize/soybean)	US-Ne1, Ne2, Ne3	GS mean	0.49	T/ET under no-till (0.49) was larger than under plow till management (0.44). Peak T/ET occurred later for soybean vs. maize
(A et al., 2022)	DBF to GRA transition	Hailaer River Basin	Annual mean	0.58	
(da Rocha et al., 2023)	GRA (ungrazed) GRA (grazed)	Rannella Flint Hills Prairie Preserve, Kansas, USA	GS mean	0.71 0.64	
(Liu & Qiao, 2023)	CRO (cotton)	Manas River Basin, Xinjiang, China	Seedling stage Budding stage Blooming and boll stage Boll opening stage Whole stage	0.34 0.61 0.81 0.51 0.61	
(da Rocha et al., 2022)	GRA	US-xKZ	GS mean	0.59	
(Bai et al., 2019)	CRO (maize)	HRB, Daman	GS mean GS peak Irrigation periods	0.74 0.83 0.63	Lower T/ET values than isotope method, similar values to lysimeter method and Shuttleworth-Wallace method
(Chen et al., 2022)	CRO (soybean) CRO (maize) CRO (wheat)	US-Br3, Ne3, Bo1 US-Ne1, CN-Yuc, Daman CN-Yuc, DE-She, US-ARM	Annual mean	0.43 0.50 0.38	
(Cao et al., 2022)	Misc.	86 FLUXNET sites	Annual mean	0.59	Similar trends as with Shuttleworth-Wallace and PT-JPL models but with lower inter-site variability
(Reavis et al., 2024)	CRO (rice)	US-HRC, HRA	GS mean	0.47	Lower T/ET with alternate wetting and drying vs. delayed continuous flooding at US-HRC, but the opposite for US-HRA
(Ma et al., 2020)	SAV GRA	US-Ton US-Var	GS mean with regular (95%) regression (with 80% quantile regression)	0.39 (0.61) 0.47 (0.65)	Both regular and 80% quantile regression estimates lower than with the SB17 method. Estimate magnitudes were regular < 80% quantile < SB17
(Raghav et al., 2022)	CRO (wheat)	GRL-FLUXNET sites 1, 2, and 3	GS mean	0.54	Lower T/ET estimates than with SK10 or TEA18 methods
(Scott et al., 2021)	DBF GRA	US-CMW US-Wkg	Annual mean	0.56 0.35	Lowest T/ET estimates in the summer compared to SB17, TEA18, and LI19 methods
(Zhou et al., 2018)	GRA CRO (maize) OSH	HRB, Arou HRB, Daman HRB, Huyanglin	GS mean	0.55 0.63 0.55	
(Jiang et al., 2020)	CRO (wheat)	CH-Oe2, US-ARM, FR-Grl	Annual mean	0.65	



	CRO (rice) CRO (soybean) CRO (maize)	US-Twt, JAN-MSE US-Ne2, Ne3, CRT  FR-Grl, IT-Bci, US-Ne1		0.57 0.60 0.67	
(Xue et al., 2023)	CRO EBF ENF DBF GRA MF OSH SAV WSA Misc.	10 sites 6 sites 13 sites 9 sites 11 sites 1 site 2 sites 2 sites 3 sites All (57 sites)	Annual mean	0.21 0.52 0.52 0.55 0.56 0.39 0.23 0.57 0.45 0.44	Across all ecosystems, T/ET from ZH16 and TSEB were lower than estimated from TSEB-SM and TEA18 methods
(Perez-Quezada et al., 2024)	DBF WET	CL-SDF CL-SDP	Annual mean	0.46 0.49	
(Sun et al., 2020)	DBF MF ENF OSH	Mount Gongga, Qinghai-Tibetan Plateau	Annual mean (uWUE estimated with $R_{net}$ in place of VPD)	0.47 0.48 0.50 0.35	
(Wu & Wang, 2025)	GRA	HRB, Arou	GS mean	0.67	Results matched well with the Soil Plant Atmosphere Continuum model
(Zhang et al., 2025a)	CRO (misc.)	US-ARM, CRT, Twt, Tw2, Tw3 IT-BCi, CA2 DE-Seh, RuS, Kli, Geb FR-Gri, FI-Jok, DK-Fou, CH-Oe2, BE-Lon	GS mean	0.48	Lower than TEA18 values (0.66). Both methods estimated the highest values from maize while ZH16 estimated the lowest values from rapeseed and TEA18 from paddy rice
(Zhang et al., 2025b)	OSH	HRB, Sidaoqiao	GS mean		ZH16 estimates agreed well with sap flow values and the two-source Penman-Monteith model. ZH16 had higher estimates than the two-source Shuttleworth and Wallace (SW) and simplified SW models
(Zheng et al., 2025)	Misc.	72 flux sites	Annual mean		Similar but slightly lower values across ecosystems when compared to SIF-driven semi-mechanistic and hybrid models
(Song et al., 2023b)	CRO	HRB, Daman	GS trend		Estimates from one GS agreed well with the TSEB-SM informed by satellite soil moisture data
(Song et al., 2022)	GRA CRO	HRB, Arou HRB, Daman	GS trend		Estimates from four GS were consistently lower than when compared to the TSEB-SM informed by surface soil moisture data
(Song et al., 2023a)	CRO	HRB, Daman	GS trend		Estimates from two GS were consistently lower than when compared to the TSEB-



					SIF. Trends followed canopy stomatal conductance
(Song et al., 2021)	GRA CRO	HRB, Arou HRB, Daman	GS trend		Seasonal trends and values of T/ET agreed well with the LSTR model (a RS-based method using land surface temperature reconstruction)
(Liu et al., 2022a)	CRO (maize)	HRB, Daman	GS trend		Similar trends as a remote sensing trapezoid-based estimate informed by LAI and NDVI values. Lower values when compared to isotopes and TEA18
(Bu et al., 2021)	CRO DBF EBF ENF WSA GRA	US-Ne1, Ne2, Ne3, ARM US-Wcr, MMS, DE-Hai AU-Tum CA-Qfo, FI-Hyy US-Wkg US-Var, SRM, AT-Neu, IT-Mbo	Annual trend		Consistently underestimated across CRO, DBF, EBF, ENF, WSA, and GRA sites when compared to TSEB model estimates
(Bu et al., 2024)	GRA SAV	ES-BB, CN-Du2, US-Var, Wkg ES-LM2, US-SRM	Annual trend		Estimates compared well with the CSIF (two-source RS model) when it was modelled with GPP and soil water content data
(Jin et al., 2022)	DBF ENF	DE-Hai, DK-Sor, IT-Col, US-MMS, Wcr CA-Qfo, DE-Tha, IT-Lav, Ren, RU-Fyo, US-GLE, NR1	Annual trend		Similar trends and values when compared to an ecosystem level conductance photosynthesis model using LAI and SWC across all sites
(MacBean et al., 2020)	ENF GRA OSH	US-Fuf, Vcp US-SRM, SRG, Wkg US-Whs	Annual trend		Similar trends and values for the ENF sites when compared to a soil hydrology-based model. The GRA and OSH sites showed similar trends but lower values compared to SB17 estimates
(Cui et al., 2024)	CRO (kiwi)	Pujiang County, Chengdu Plain, China	Annual trend		Generally lower values than those estimated from an LAI informed conductance model however mid-GS values were similar
(Yu et al., 2022)	CRO DBF EBF ENF GRA WSA	DE-RuS, Seh, US-CRT, Ne1, Ne2, Ne3 CA-Oas, DE-Hai, FR- Fon, US-Ha1, UMB FR-Pue, IT-Cpz CA-NS3, DE-Obe, NL- Loo, US-NR1 DE-Gri, US-Arb, Arc, Goo, SRG US-SRM, Ton	Annual trend		Similar trends when compared to an EC/LSM-based method across global PFTs and TEA18
(Gnanamoorthy et al., 2024)	EBF	Yunnan Province, China	Annual trend		Similar values and trends to an EC/LSM-based method
(Hao et al., 2024)	ENF	CA-LP1	Annual trend		Lower estimates than from TEA18 but both showed similar trends



(Li et al., 2024e)	ENF	CA-Ca3	Annual trend		Lowest T/ET values when compared to TEA18 and EE22 estimates
(Zheng et al., 2024)	CRO (wheat)	Zhao Xian, Shijiazhuang City, Hebei Province, China	Annual trend		Similar estimates to TEA18
(Räsänen et al., 2022)	SAV	Welgegund, South Africa	Annual trend		Lower values than TEA18, similar values to BH16
(Tong et al., 2019)	CRO (maize)	HRB, Daman	Annual trend		Lower than values from the isotope method
(Li et al., 2024c)	WET	Qixing River National Nature Reserve, Heilongjiang Province, China	Annual trend		E dominated ET, T peaked midday in accordance with GPP

## 6.2 LI19

Table A2: Studies that have used the ecosystem conductance partitioning method by Li et al. (2019) to calculate the transpiration to evapotranspiration ratio (T/ET). The timescales used in the T/ET calculations are listed as well as any comparisons to other ET partitioning methods. Locations are listed by FLUXNET site IDs when applicable, for any non-FLUXNET sites, the location is listed in accordance to how it was reported in the methods of each study. The plant functional types (PFT) of the ecosystems are identified with CRO: cropland, GRA: grassland, DBF: deciduous broadleaf forest, ENF: evergreen needleleaf forest, EBF: evergreen broadleaf forest, MF: mixed forest, SAV: savanna, WSA: woody savanna, OSH: shrubland, BSV: bare sparse vegetation, WET: wetland. GS: growing season, LAI: leaf area index. Methods: ZH16: Zhou et al. (2016), LI19: Li et al. (2019), PP18: Perez-Preigo et al. (2018), TEA18: Nelson et al. (2018), SK10: Scanlon & Kustas (2010), SB17: Scott & Biederman (2017).

Reference	PFT	Location	Calculation	T/ET	Notes
(Li et al., 2019)	ENF	CA-Qfo, SF1, SF2, DE-Obe, FI-Hyy, FR-LBr, IT-Ren, Sro, NL-Loo, US-NR1	Annual mean	0.75	
	CRO	DE-Geb, Kli, FR-Gri, US-ARM, Ne1, Ne2, Ne3		0.62	
	GRA	AT-Neu, DE-Gri, US-AR1, AR2, SRG, Var, Wkg		0.56	
	DBF	IT-Col, DE-Hai, ZM-Mon		0.80	
	EBF	BR-Sa3		0.54	
	WSA	US-SRM, Ton		0.61	
(Hu & Lei, 2021)	CRO (wheat) CRO (maize)	Weishan, North China Plain	GS mean	0.59 0.44	Values and dynamics of T/ET compared poorly to the two-stage theory of bare soil E. For maize, similar values as ZH16 and smaller values compared to SB17, SK10, and TEA18. Wheat LI19 estimates were greater than PP18, ZH16, and SK10 and smaller than SB17 and TEA18



(Ohkubo et al., 2023)	WET	Kalimantan, Indonesia	Annual mean	0.56	Drained and slightly drained swamps had higher T/ET than the burned degraded swamp (0.21)
(Scott et al., 2021)	DBF GRA	US-CMW US-Wkg	Annual mean	0.36 0.78	Lowest DBF values in the spring/fall compared to ZH16, TEA18, and SB17
(Nie et al., 2021)	DBF EBF ENF MF Misc.	11 sites 3 sites 19 sites 3 sites All (36) forest sites	Annual mean	0.73	
(Maes et al., 2020)	Misc.	86 global FLUXNET sites	Annual mean	0.66	Lower than an LAI-based method (Wei et al., 2017) which showed an inter-site mean of 0.69
(Restrepo-Coupe et al., 2023)	DBF	Tapajos national forest, Brazil	From daily T and E totals	0.86	Seasonal trends correlated with incoming shortwave radiation and LAI. Drought decreased T/ET while a wet La Niña period increased estimates

### 6.3 PP18

Table A3: Studies that have used the conductance partitioning model by Perez-Preigo et al. (2018) to calculate the transpiration to evapotranspiration ratio (T/ET). The timescales used in the T/ET calculations are listed as well as any comparisons to other ET partitioning methods. Locations are listed by FLUXNET site IDs when applicable, for any non-FLUXNET sites, the location is listed in accordance to how it was reported in the methods of each study. The plant functional types (PFT) of the ecosystems are identified with CRO: cropland, GRA: grassland, DBF: deciduous broadleaf forest, ENF: evergreen needleleaf forest, EBF: evergreen broadleaf forest, MF: mixed forest, SAV: savanna, WSA: woody savanna, OSH: shrubland, BSV: bare sparse vegetation, WET: wetland. GS: growing season, LAI: leaf area index, HRB: Heihe River Basin. Methods: ZH16: Zhou et al. (2016), LI19: Li et al. (2019), PP18: Perez-Preigo et al. (2018), TEA18: Nelson et al. (2018), SK10: Scanlon & Kustas (2010), SB17: Scott & Biederman (2017).

Reference	PFT	Location	Calculation	T/ET	Notes
(Perez-Priego et al., 2018)	SAV	ES-LMa	GS range	0.20-0.40	Diurnal trends are consistently lower than those from SK10
(Nelson et al., 2020)	Misc.	251 FLUXNET sites	Annual mean	0.45	Similar, slightly lower than T/ET estimates from ZH16 method, lower than TEA18 estimates
(Hu & Lei, 2021)	CRO (wheat)	Weishan, North China Plain	GS mean	0.46	Lower T/ET values and different 14-day trends than the two-stage theory of bare soil evaporation, lower estimates than SB17, SK10, LI19, ZH16, and TEA18
(Liu et al., 2022a)	CRO (maize)	HRB, Daman	GS mean		Lowest T/ET values compared to estimates made with ZH16, TEA18, isotope-based, LAI-based, and remote sensing trapezoid based methods



(Lowry et al., 2021)	WET (native) WET (swamp) ENF	Bribie Island, Queensland, Australia	Annual mean	0.34 0.23 0.55	
(Reich et al., 2024)	WSA	US-Mpj	GS mean	0.60	Higher T/ET estimate than sap-flow but lower than SB17b

#### 6.4 TEA18

Table A4: Studies that have used the Transpiration Estimation Algorithm by Nelson et al. (2018) to calculate the transpiration to evapotranspiration ratio (T/ET). The timescales used in the T/ET calculations are listed as well as any comparisons to other ET partitioning methods. Locations are listed by FLUXNET site IDs when applicable, for any non-FLUXNET sites, the location is listed in accordance to how it was reported in the methods of each study. The plant functional types (PFT) of the ecosystems are identified with CRO: cropland, GRA: grassland, DBF: deciduous broadleaf forest, ENF: evergreen needleleaf forest, EBF: evergreen broadleaf forest, MF: mixed forest, SAV: savanna, WSA: woody savanna, OSH: shrubland, BSV: bare sparse vegetation, WET: wetland. GS: growing season, LAI: leaf area index, HRB: Heihe River Basin, TSEB: two source energy balance model, TSEB-SM: TSEB aided by soil moisture. Methods: ZH16: Zhou et al. (2016), LI19: Li et al. (2019), PP18: Perez-Preigo et al. (2018), TEA18: Nelson et al. (2018), SK10: Scanlon & Kustas (2010), SB17: Scott & Biederman (2017).

Reference	PFT	Location	Calculation	T/ET	Notes
(Nelson et al., 2018)	DBF	FR-Hes	GS mean	0.77	T/ET estimates agree well with values from the sap flow method. When applied in 2 ENF sites (DE-Tha and FI-Hyy), TEA18 estimates fall within the range of T values predicted from 3 ecosystem models
(D'Acunha et al., 2024)	CRO (soybean)	Amazon agriculture, Cerrado agriculture Lucas do Rio Verde, Cerrado agriculture Jaciara	From annual T, ET totals	0.61	Higher T/ET estimates than with ZH16
	DBF	Amazon forest Tanguro, Amazon forest Sinop, Pantanal forest		0.60	
	GRA	Amazon pasture, Pantanal pasture		0.67	
	WSA	Cerrado Campo sujo		0.71	
	Misc.	All Mato Grosso, Brazil sites (from above)		Annual mean 0.63	
(Nelson et al., 2020)	DBF	251 FLUXNET sites	Annual mean	0.70	Higher T/ET estimates than with ZH16 and PP18
	GRA			0.67	
	ENF			0.62	
	Misc.			0.77	
			Peak seasonal	0.83	
(Hu & Lei, 2021)	CRO (wheat)	Weishan, North China Plain	GS mean	0.77	T/ET values and trends agreed well with the two-stage theory of bare soil
	CRO (maize)			0.71	



					evaporation, higher estimates than SB17, SK10, LI19, ZH16, and PP18 (for wheat)
(Paul-Limoges et al., 2022)	CRO (wheat) CRO (barley)	CH-Oe2 CH-Oe2	GS mean	0.73 0.75	Increased diurnal and seasonal T/ET trends and values than ZH16 method
(Li et al., 2024e)	ENF	CA-Ca3	Annual mean	0.69	Similar T/ET trends and values to EE22 method, consistently higher than ZH16 estimates
(Liu et al., 2022a)	CRO (maize)	HRB, Daman	GS mean	>0.85	Higher T/ET values than estimates made with ZH16, PP18, isotope-based, LAI-based, and remote sensing trapezoid based methods
(Räsänen et al., 2022)	SAV	Welgegund Research Station, South Africa	GS mean	0.61	Daily T/ET values and seasonal trends consistently higher than with ZH16 and BH16
(Raghav et al., 2022)	CRO (wheat)	GRL-FLUXNET sites 1, 2, and 3	GS mean	0.76	Similar, slightly higher T/ET estimates than with SK10, higher estimates than ZH16 method
(Scott et al., 2021)	DBF GRA	US-CMW US-Wkg	Annual mean	0.74 0.46	Similar T/ET values to SB17 with higher estimates than ZH16 and LI19 methods
(Wang et al., 2022)	CRO (rubber)  DBF	Northern rubber: Chachoengsao Province, TH Southern rubber: Nakhon Si Thammarat Province, TH Ratchaburi Province, TH	Annual mean	0.78  0.72	
(Xue et al., 2023)	CRO EBF ENF DBF GRA MF OSH SAV WSA Misc.	10 sites 6 sites 13 sites 9 sites 11 sites 1 site 2 sites 2 sites 3 sites All (57 sites)	Annual mean	0.33 0.78 0.74 0.70 0.75 0.51 0.34 0.76 0.67 0.61	Across all ecosystems, T/ET from TEA18 and TSEB-SM were higher than when estimated from ZH16 and TSEB
(Kibler et al., 2023)	DBF  WSA	US-CMW  US-SRM	GS median	0.87 - 0.92 0.72 - 0.80	
(El-Madany et al., 2021)	SAV	ES-LMa, LM1, LM2	From annual T, ET totals	0.69	Higher T/ET in SAV fertilized with nitrogen (0.70) and SAV fertilized with nitrogen and phosphorus (0.71) than control SAV (0.65)
(Zhang et al., 2025a)	CRO (misc.)	US-ARM, CRT, Twt, Tw2, Tw3 IT-BCi, CA2 DE-Seh, RuS, Kli, Geb	GS mean	0.66	Higher than ZH16 values (0.48). Both methods estimated the highest values from maize while ZH16 estimated the lowest values from rapeseed and TEA18 from paddy rice



		FR-Gri, FI-Jok, DK-Fou, CH-Oe2, BE-Lon			
(Bastos Campos et al., 2025)	CRO (vineyard)	Kaltern-Caldaro, South Tyrol, Northern Italy	GS mean	0.78	Similar but slightly higher estimates than with sap flow measurements
(Liu et al., 2025)	OSH	Yanchi Research Station, Beijing, China	Annual mean	0.59	TEA18 estimates compared well with sap flow measurements. EE22 estimates were ~20% lower than TEA18
(Yang et al., 2025a)	CRO (maize, wheat)	Weishan, North China Plain	GS trend		T dominated ET during the GS. TEA18 estimates agreed well with an ecohydrological model (Weishan model)
(Hao et al., 2024)	ENF	CA-LP1	Annual trend		Consistently higher than ZH16 estimates although both methods had similar trends
(Zheng et al., 2024)	CRO (wheat)	Zhao Xian, Shijiazhuang City, Hebei Province, China	Annual trend		Similar estimates to ZH16
(Yu et al., 2022)	CRO DBF EBF ENF GRA WSA	DE-RuS, Seh, US-CRT, Ne1, Ne2, Ne3 CA-Oas, DE-Hai, FR-Fon, US-Ha1, UMB FR-Pue, IT-Cpz CA-NS3, DE-Obe, NL-Loo, US-NR1 DE-Gri, US-Arb, Arc, Goo, SRG US-SRM, Ton	Annual trend		Similar trends when compared to an EC/LSM-based method across global PFTs and ZH16

### 6.5 SK10

585 Table A5: Studies that have used the Flux Variance Similarity partitioning method by Scanlon & Kustas (2010) to calculate the transpiration to evapotranspiration ratio (T/ET). The timescales used in the T/ET calculations are listed as well as any comparisons to other ET partitioning methods. Locations are listed by FLUXNET site IDs when applicable, for any non-FLUXNET sites, the location is listed in accordance to how it was reported in the methods of each study. The plant functional types (PFT) of the ecosystems are identified with CRO: cropland, GRA: grassland, DBF: deciduous broadleaf forest, ENF: evergreen needleleaf forest, EBF: evergreen broadleaf forest, MF: mixed forest, SAV: savanna, WSA: woody savanna, OSH: shrubland, BSV: bare sparse vegetation, WET: wetland. GS: growing season, LAI: leaf area index, HRB: Heihe River Basin, TSEB: two source energy balance model, LSM: land surface model. Methods: ZH16: Zhou et al. (2016), LI19: Li et al. (2019), PP18: Perez-Preigo et al. (2018), TEA18: Nelson et al. (2018), SK10: Scanlon & Kustas (2010), SB17: Scott & Biederman (2017).

Reference	PFT	Location	Calculation	T/ET	Notes
(Hu & Lei, 2021)	CRO (wheat) CRO (maize)	Weishan, North China Plain	GS mean / const ppm	0.55 0.70	T/ET values agreed with values from the two-stage theory of bare soil E and TEA18 for maize, but underestimated wheat comparatively. Values for maize



					estimations were greater than ZH16, LI19, and SB17 methods and greater than PP18 and ZH16 for wheat.
(Raghav et al., 2022)	CRO (wheat)	GRL-FLUXNET sites 1, 2, and 3	GS mean / const ratio	0.75	Similar T/ET estimates with TEA18 method, higher estimates than ZH16 method
(Wang et al., 2016a)	GRA	Xilin River watershed, Inner Mongolia, China	GS mean / const ppm	0.65	Winter grazing and heavy grazing saw lower T/ET than ungrazed treatments
(Schreiner-McGraw et al., 2022)	CRO (pistachio) CRO (almond)	US-PSL, PSH US-ASL, ASM, ASH	Annual mean / const ppm	0.79 0.65	
(De Haan et al., 2021)	CRO (alfalfa) CRO (maize)	Hopewell Creek Watershed, Ontario, Canada	GS mean / const ppm	0.58 0.71	Alfalfa T/ET showed less seasonality than the maize
(Gao et al., 2024)	CRO (wheat)	Zhangye Oasis, Gansu Province, China	GS mean / const ratio	0.55	
(Ferrara et al., 2024)	CRO (watermelon)	CREA-AA Research Unit, Italy	From GS T, E totals / const ppm	0.51	
(Rana et al., 2018)	CRO (fava bean) CRO (wheat)	CREA-AA Research Unit, Italy	Emergence stage (flowering stage) / const ppm	0.25 (0.43) 0.30 (0.37)	
(Anupoju et al., 2024)	CRO (rice)	Vizianagaram, Andhra Pradesh, India	GS mean / const ppm	0.70	Similar T/ET values as FAO Dual Kc-ETo and Priestley-Taylor methods
(Scanlon et al., 2019; Sulman et al., 2016)*	DBF	US-MMS	GS mean / optimum	0.82	Compared to 0.84 during a severe drought year. Similar T trends with slightly lower values as a sub-canopy based method *Sulman et al. (2016) removed low-frequency data using wavelet analysis while Scanlon et al. (2019) used a moving mean window. Both studies used the same data and came to a similar conclusion regarding T/ET estimates
(Peddinti & Kambhammettu, 2019)	CRO (citrus orchard)	Goregone village, Vidarbha, India	Annual mean / const ppm	0.66	Similar T/ET from SIMDualKc model
(Wagle et al., 2021a)	CRO (canola)	Grazinglands Research Laboratory, USDA-ARS	GS mean / const ratio	~0.70	No significant difference in T/ET between till and no-till fields
(Wagle et al., 2021b)	CRO (canola)  CRO (wheat)  CRO (soybean) CRO (maize)	Grazinglands Research Laboratory, USDA-ARS	Peak growth mean / const ppm, const ratio, optimum, linear, sqrt	0.76-0.88 0.75-0.88 0.80-0.86 0.78-0.90	Range dependent on which WUE algorithm was used. Const_ppm, const_ratio, and optimum models were consistent with each other and there was a higher T/ET for linear and sqrt models in wheat and canola



	CRO (sorghum)			0.66-0.88	
(Shveytser et al., 2022)	DBF ENF WET Misc.	US-PFk, PFL, PFm, PFn, PFc, PFp, PFq, PFs, PFi, PFj US-PFb, PFg, PFh, PFt US-PFd, PFe, PFr All sites	GS mean / const ratio	0.54 0.53 0.46 0.52	
(Wagle et al., 2020)	CRO (alfalfa)	Grazinglands Research Laboratory, USDA-ARS	GS mean / const ratio	~0.80	
(Wagle et al., 2023)	CRO (wheat) CRO (canola)	Grazinglands Research Laboratory, USDA-ARS	GS mean / const ppm, const ratio, linear, sqrt, optimum	0.64-0.89 0.59-0.85	Range dependent on WUE algorithm used
(Liu et al., 2022b)	GRA	Bange, Tibetan Plateau	Annual mean / const ratio	0.34	
(Anderson et al., 2018)	CRO (peach orchard)	San Joaquin Valley, California, USA	GS mean / const ppm, const ratio, linear, sqrt	0.48-0.84	Range dependent on WUE algorithm used
(Wang et al., 2016b)	GRA/URB	Broadmead site, New Jersey, USA	Annual mean / const ratio	>0.70	Similar seasonal and diurnal patterns as NOAH LSM but decreased summer T/ET from SK10
(Scanlon & Kustas, 2012)	CRO (corn)	OPE <sup>3</sup> , USDA-ARS	Crop maturity / const ratio	0.70-0.80	
(Borges et al., 2024)	DBF	Campina Grande, State of Paraíba, Brazil Serra Negra, State of Rio Grande do Norte, Brazil	Rainy season / const ratio	0.65	Slightly higher T/ET for sparse vegetation cover (0.67) vs. dense vegetation cover (0.64)
(Li et al., 2024b)	DBF/URB	Nankai University, Tianjin, China	GS mean / const ppm, const ratio, sqrt, optimum, linear	0.80-0.88	Range dependent on WUE algorithm used, similar seasonal trends for const ppm, const ratio, sqrt, and optimum. Linear algorithm had higher T/ET values
(Klosterhalfen et al., 2019b)	CRO (wheat) ENF	DE-Rus DE-RuW	Annual median / const ppm	0.77-0.91 0.84	
(Kustas et al., 2018)	CRO (vineyard)	Borden Ranch, California, USA	June mean	0.83	Compared to sap-flow measurements of 0.80
(Wang et al., 2024b)	CRO (poplar plantation)	MinQuan site, Henan Province, China	July, Aug, Sep mean / optimum	0.67	Lower T/ET estimates than TH08 (0.78) method, and higher than the ZN22 (0.63) method
(Gao et al., 2025)	CRO (wheat)	HRB, Zhangye	GS mean / const ratio	0.55	E dominated when looking at annual means
(Wang et al., 2025)	CRO (evergreen plantation)	Jiyuan (JY2) Jinzhai Jianping (JP1, JP2) MinQuan	GS mean, all sites: Const ppm Const ratio	0.63 0.64	Deciduous plantations had more consistent T/ET values across model runs compared to the evergreen plantation



	CRO (deciduous plantation)	Jiyuan (JY1) Henan Province, China	Linear Sqrt Optimum	0.78 0.70 0.65	
(Paciolla et al., 2025)	CRO (vineyard)	California, USA	Mean midday peaks, const ratio	~0.60	Much lower than estimates from ZN22, TH08 (midday peaks ~100%). FEST-2-EWB (a two-source LSM) agreed well with ZN22 and TH08 while TSEB produced the highest estimates from all methods
(Scanlon & Kustas, 2010)	CRO (maize)	Maryland, USA	Annual trend		SK10 was able to identify changes in T/ET after precipitation and T estimates followed LAI trends
(Skaggs et al., 2018)	CRO (peach)	San Joaquin Valley, California, USA	GS trend		T/ET decreased under well-watered conditions
(Deb Burman et al., 2022)	WET DBF	Tamil Nadu, India Assam, northeast India	Annual trend		WET had higher T/ET during the GS but did not show seasonal dynamics. The DBF had higher T/ET from September to December and showed seasonal variability
(Shih et al., 2025)	EBF ENF	Lien-Hua-Chih, Taiwan Chi-Lan, Taiwan	Daily trend		Higher midday peak T/ET in the EBF with peak values occurring between 12-2pm (local time) while the ENF peaked early and values decreased from 6am-3pm
(Carneiro et al., 2025)	OSH	Dense caatinga Sparse caatinga Northeastern Brazil	Annual mean		Sparse caatinga with more exposed rocky outcrops and bare soil had lower T/ET than the dense caatinga
(Klosterhalfen et al., 2019a)	ENF DBF CRO GRA	4 sites across Europe, 1 site in Oregon, USA 2 sites in Europe 2 sites in Europe 3 sites in Europe	Annual trend		Consistently lower T estimates than TH08 across all ecosystems. SK10 showed no clear difference in T/ET across biomes
(Good et al., 2014)	CRO (pistachio and almond)	Mpala Research Center, Kenya	GS trend		Similar to the isotope method during peak GS, but showed T before any green leaves had sprouted and continued after senescence
(Kustas et al., 2019a)	CRO (vineyard)	California, USA	GS trend		T estimates agreed well with results from the micro-Bowen ratio method
(Rana et al., 2019)	CRO (vineyard)	Mazaro River Basin, Sicily	Annual trend		T estimates were higher than results from sap flow method
(Song et al., 2018)	CRO (maize)	HRB, Daman	GS trend		T/ET values were 10% lower than results from a MODIS-based dual temperature difference model
(Kustas et al., 2019b)	CRO (vineyard)	California, USA	GS trend		Higher peak seasonal values than the TSEB and TSEB-LAI



## 6.6 SB17

Table A6: Studies that have used the linear regression-based partitioning method by Scott & Biederman (2017) to calculate the transpiration to evapotranspiration ratio (T/ET). The timescales used in the T/ET calculations are listed as well as any comparisons to other ET partitioning methods. Locations are listed by FLUXNET site IDs when applicable, for any non-FLUXNET sites, the location is listed in accordance to how it was reported in the methods of each study. The plant functional types (PFT) of the ecosystems are identified with CRO: cropland, GRA: grassland, DBF: deciduous broadleaf forest, ENF: evergreen needleleaf forest, EBF: evergreen broadleaf forest, MF: mixed forest, SAV: savanna, WSA: woody savanna, OSH: shrubland, BSV: bare sparse vegetation, WET: wetland. GS: growing season, LSM: land surface model. Methods: ZH16: Zhou et al. (2016), LI19: Li et al. (2019), PP18: Perez-Preigo et al. (2018), TEA18: Nelson et al. (2018), SK10: Scanlon & Kustas (2010), SB17: Scott & Biederman (2017).

Reference	PFT	Location	Calculation	T/ET	Notes
(MacBean et al., 2020; Scott and Biederman, 2017)*	OSH SAV GRA	US-Whs US-SRM US-SRG, Wkg	GS mean	0.44 0.62 0.51	Similar annual T/ET trends with higher values than estimates made with the ZH16 method *Scott and Biederman (2017) was the method establishment while MacBean et al. (2020) compared outputs to an LSM, which showed lower values and different trends to SB17
(Hu & Lei, 2021)	CRO (wheat) CRO (maize)	Weishan, North China Plain	GS mean	0.70 0.64	Greater maize T/ET values than ZH16 and LI19, smaller values than SK10, TEA18, and the two-stage theory of bare soil evaporation. For wheat, greater values than PP18, ZH16, SK10, and LI19 and smaller values than TEA18
(Ma et al., 2020)	SAV GRA	US-Ton US-Var	GS mean	0.74 0.66	Higher T/ET values than ZH16 with regular (95%) and 80% quantile regression
(Scott et al., 2021)	DBF	US-CMW	Annual mean	0.40	Similar values to TEA18 but higher monthly values than ZH16 and LI19
(Sun & Versegghy, 2019)	OSH	US-Whs	Summer mean	0.49	
(Eichelmann et al., 2022)	WET	US-TW1, TW4, MYB, Sne	Annual trend		Lower values than EE22 for wetland sites with increased standing water. EE22 results compared better with leaf-level T measurements

## 6.7 Methods with limited testing

Table A7: Studies that have used various partitioning methods found from the literature review to calculate the transpiration to evapotranspiration ratio (T/ET). The timescales used in the T/ET calculations are listed as well as any comparisons to other ET partitioning methods. Locations are listed by FLUXNET site IDs when applicable, for any non-FLUXNET sites, the



610 location is listed in accordance to how it was reported in the methods of each study. The plant functional types (PFT) of the ecosystems are identified with CRO: cropland, GRA: grassland, DBF: deciduous broadleaf forest, ENF: evergreen needleleaf forest, EBF: evergreen broadleaf forest, MF: mixed forest, SAV: savanna, WSA: woody savanna, OSH: shrubland, BSV: bare sparse vegetation, WET: wetland. GS: growing season, TSEB: two source energy balance model, LSM: land surface model. Methods: ZH16: Zhou et al. (2016), LI19: Li et al. (2019), PP18: Perez-Preigo et al. (2018), TEA18: Nelson et al. (2018), 615 SK10: Scanlon & Kustas (2010), SB17: Scott & Biederman (2017), BH16: Berkelhammer et al. (2016), TH08: Thomas et al. (2008), ZN22: Zahn et al. (2022), SB17b: Reich et al. (2024), EE22: Eichelmann et al. (2022). Method types: uWUE: underlying water use efficiency, HF: high frequency, LR: linear regression, ML: machine learning.

Method	Method type	Reference	PFT	Location	Calculation	T/ET	Notes
BH16	uWUE	(Berkelhammer et al., 2016)	ENF	US-NR1, MEF	Annual mean	0.56	Trends agree with isotopic approach on the synoptic scale
BH16	uWUE	(Räsänen et al., 2022)	SAV	Welgegund Research Station, South Africa	GS mean	0.46	Daily T/ET values lower than with TEA18 and ZH16 methods
BH16	uWUE	(Dukat et al., 2023)	ENF	Mezyk and Tuczno, Poland	GS mean	0.75	Much higher T/ET estimate than with sap flow method (0.48)
BH16	uWUE	(Knowles et al., 2023)	ENF	US-NR1, GLEES			31% decrease in T relative to ET after a bark beetle pathogen outbreak while T recovered quicker than ET post outbreak
BH16	uWUE	(Cammalleri et al., 2024)	CRO (almond, olive, vineyard)	California, USA			Similar T/ET estimates to various TSEB models (PT, PM, 2T)
TH08	HF	(Wang et al., 2024b)	CRO (poplar plantation)	MinQuan site, Henan Province, China	July, Aug, Sep mean	0.78	TH08 estimated value was higher than SK10 (0.67), while ZN22 estimated value was the lowest of the three methods
ZN22	HF					0.63	
ZN22	HF	(Zahn et al., 2022)	GRA	Mpala Research Center, Kenya Wind River Experimental forest, USA	Dry period mean	0.51	Similar seasonal trends as TH08, SK10, and the isotopic method
			ENF		Summer mean	0.62	
ZN22	HF	(Amaro Medina et al., 2025)	WET	Sandhill Fen, Alberta, Canada	GS mean	~0.70	



SK10/ ZN22/ TH08	HF (all)	(Zahn & Bou-Zeid, 2024)	Misc.	47 NEON sites	Winter mean Summer mean	0.5 0.7	TH08 and ZN22 estimated higher values in the summer when compared to SK10, ZN22b and TH08b
TH08/ ZN22/ SK10	HF (all)	(Paciolla et al., 2025)	CRO (vineyard)	California, USA	Mean midday peaks	~1.0	ZN22 and TH08 had higher estimates than SK10 (midday peaks ~60%). FEST-2-EWB (a two-source LSM) agreed well with ZN22 and TH08 while TSEB produced the highest estimates from all methods
ZH16 & SB17*	uWUE/ LR	(Yuan et al., 2021)	GRA/ WSA	US-SRG / US-SRM	GS mean / uWUE and SB17 methods averaged	0.68	*ZH16 was corrected based on SB17 estimates and results are a combination of methods Maximum T/ET occurred in October (0.84) and minimum occurred in December (0.14). Individual monthly estimates were lower with SB17 than with ZH16.
SB17b	LR	(Reich et al., 2024)	GRA OSH SAV WSA ENF	US-Seg US-Ses US-Wjs US-Mpj US-Vcp, Vcm, Vcs	GS mean	0.88 0.84 0.94 0.87 0.93	Low elevation sites (US-Seg, Ses) agreed well with SB17, the mid- and high-elevation sites did not agree with SB17 estimates. WSA values were higher with SB17b than PP18
EE22	ML	(Eichelmann et al., 2022)	WET	US-TW1, TW4, MYP, Sne	Annual trend		T/ET trends agreed well with leaf-level T measurements and followed GEP patterns, estimates were higher than SB17
EE22	ML	(Liu et al., 2025)	OSH	Yanchi Research Station, Beijing, China	Annual mean		Estimates were ~20% lower than TEA18 and sap flow values
EE22	ML	(Li et al., 2024e)	ENF	CA-Ca3	Annual trend		Trends and values agreed well with TEA18, which were both higher than ZH16

### Data availability

620 No datasets were used in this article



### **Author contributions**

EGC and EE were involved in conceptualization, EGC performed the analysis used to create figures and tables and prepared the manuscript. All co-authors contributed to writing.

### **Competing interests**

625 The authors declare that they have no conflict of interest.

### **Financial support**

The research was funded from a University College Dublin School of Biology and Environmental Science Demonstratorship.



## 630 References

- A, Y., Wang, G., Hu, P., Wang, L., Xue, B., and Shrestha, S.: Modification and upscaling of S–W model based on vertical distributions of soil moisture and vegetation root biomass, *Environ. Res.*, 208, <https://doi.org/10.1016/j.envres.2022.112765>, 2022.
- Addington, R. N., Mitchell, R. J., Oren, R., and Donovan, L. A.: Stomatal sensitivity to vapor pressure deficit and its relationship to hydraulic conductance in *Pinus palustris*, *Tree Physiol.*, 24, 561–569, 2004.
- 635 Amaro Medina, D., Clark, M. G., and Carey, S. K.: Multi-Year Evapotranspiration and Energy Dynamics of a Reclaimed Fen in the Athabasca Oil Sands Region, *Hydrol. Process.*, 39, <https://doi.org/10.1002/hyp.70247>, 2025.
- Anderson, M., Gao, F., Knipper, K., Hain, C., Dulaney, W., Baldocchi, D., Eichelmann, E., Hemes, K., Yang, Y., Medellin-Azuara, J., and Kustas, W.: Field-scale assessment of land and water use change over the California delta using remote sensing, *Remote Sens. (Basel)*, 10, <https://doi.org/10.3390/rs10060889>, 2018.
- 640 Anupju, V., Kambhammettu, B. V. N. P., and Peddinti, S. R.: Comparative analysis of FAO dual Kc, Priestley-Taylor and flux variance similarity methods in partitioning evapotranspiration from flood-irrigated rice fields, *Irrigation and Drainage*, <https://doi.org/10.1002/ird.3039>, 2024.
- Bai, Y., Li, X., Zhou, S., Yang, X., Yu, K., Wang, M., Liu, S., Wang, P., Wu, X., Wang, X., Zhang, C., Shi, F., Wang, Y., and Wu, Y.: Quantifying plant transpiration and canopy conductance using eddy flux data: An underlying water use efficiency method, *Agric. For. Meteorol.*, 271, 375–384, <https://doi.org/10.1016/j.agrformet.2019.02.035>, 2019.
- 645 Baldocchi, D. D.: Assessing the eddy covariance technique for evaluating carbon dioxide exchange rates of ecosystems: Past, present and future, *Glob. Chang. Biol.*, 9, 479–492, <https://doi.org/10.1046/j.1365-2486.2003.00629.x>, 2003.
- Baldocchi, D. D.: How eddy covariance flux measurements have contributed to our understanding of Global Change Biology, <https://doi.org/10.1111/gcb.14807>, 1 January 2020.
- 650 Bastos Campos, F., Callesen, T. O., Gonzalez, C. V., Alberti, G., Montagnani, L., Tagliavini, M., Nelson, J. A., and Zanutelli, D.: Evapotranspiration Dynamics and Partitioning in a Grassed Vineyard: Ecophysiological and Computational Modeling Approaches, *Water Resour. Res.*, 61, <https://doi.org/10.1029/2023WR035360>, 2025.
- Beer, C., Ciais, P., Reichstein, M., Baldocchi, D., Law, B. E., Papale, D., Soussana, J. F., Ammann, C., Buchmann, N., Frank, D., Gianelle, D., Janssens, I. A., Knohl, A., Köstner, B., Moors, E., Rouspard, O., Verbeeck, H., Vesala, T., Williams, C. A., and Wohlfahrt, G.: Temporal and among-site variability of inherent water use efficiency at the ecosystem level, *Global Biogeochem. Cycles*, 23, <https://doi.org/10.1029/2008GB003233>, 2009.
- 655 Berkelhammer, M., Noone, D. C., Wong, T. E., Burns, S. P., Knowles, J. F., Kaushik, A., Blanken, P. D., and Williams, M. W.: Convergent approaches to determine an ecosystem’s transpiration fraction, *Global Biogeochem. Cycles*, 30, 933–951, <https://doi.org/10.1002/2016GB005392>, 2016.
- 660 Bishop, C. M.: *Neural Networks for Pattern Recognition*, Oxford University Press, New York, 1995.



- Bonan, G. B., Lawrence, P. J., Oleson, K. W., Levis, S., Jung, M., Reichstein, M., Lawrence, D. M., and Swenson, S. C.: Improving canopy processes in the Community Land Model version 4 (CLM4) using global flux fields empirically inferred from FLUXNET data, *J. Geophys. Res.*, 116, <https://doi.org/10.1029/2010jg001593>, 2011.
- 665 Bonan, G. B., Oleson, K. W., Fisher, R. A., Lasslop, G., and Reichstein, M.: Reconciling leaf physiological traits and canopy flux data: Use of the TRY and FLUXNET databases in the Community Land Model version 4, *J. Geophys. Res. Biogeosci.*, 117, <https://doi.org/10.1029/2011JG001913>, 2012.
- Borges, C. K., Carneiro, R. G., Santos, C. A., Zeri, M., Pocza, P., Cunha, A. P. M. A., Stachlewska, I. S., and dos Santos, C. A. C.: Partitioning of water vapor and CO<sub>2</sub> fluxes and underlying water use efficiency evaluation in a Brazilian seasonally dry tropical forest (Caatinga) using the Fluxpart model, *J. South Am. Earth Sci.*, 142, <https://doi.org/10.1016/j.jsames.2024.104963>, 2024.
- 670 Breiman, L.: Random Forest, *Mach. Learn.*, 45, 5–32, <https://doi.org/10.1023/A:1010933404324>, 2001.
- Brutsaert, W.: Global land surface evaporation trend during the past half century: Corroboration by Clausius-Clapeyron scaling, *Adv. Water Resour.*, 106, 3–5, <https://doi.org/10.1016/j.advwatres.2016.08.014>, 2017.
- 675 Bu, J., Gan, G., Chen, J., Su, Y., García, M., and Gao, Y.: Biophysical constraints on evapotranspiration partitioning for a conductance-based two source energy balance model, *J. Hydrol. (Amst.)*, 603, <https://doi.org/10.1016/j.jhydrol.2021.127179>, 2021.
- Bu, J., Gan, G., Chen, J., Su, Y., Yuan, M., Gao, Y., Domingo, F., López-Ballesteros, A., Migliavacca, M., El-Madany, T. S., Gentine, P., Xiao, J., and Garcia, M.: Dryland evapotranspiration from remote sensing solar-induced chlorophyll fluorescence: Constraining an optimal stomatal model within a two-source energy balance model, *Remote Sens. Environ.*, 303, <https://doi.org/10.1016/j.rse.2024.113999>, 2024.
- 680 Cammalleri, C., Rallo, G., Agnese, C., Ciraolo, G., Minacapilli, M., and Provenzano, G.: Combined use of eddy covariance and sap flow techniques for partition of et fluxes and water stress assessment in an irrigated olive orchard, *Agric. Water Manag.*, 120, 89–97, <https://doi.org/10.1016/j.agwat.2012.10.003>, 2013.
- 685 Cammalleri, C., Anderson, M. C., Bambach, N. E., McElrone, A. J., Knipper, K., Roby, M. C., and Kustas, W. P.: Field scale partitioning of Landsat land surface temperature into soil and canopy components for evapotranspiration assessment using a two-source energy balance model, *Irrig. Sci.*, <https://doi.org/10.1007/s00271-024-00976-w>, 2024.
- Campbell, G. S. and Norman, J. M.: *An Introduction to Environmental Biophysics*, Springer New York, New York, NY, <https://doi.org/10.1007/978-1-4612-1626-1>, 1998.
- 690 Cao, L., Bala, G., Caldeira, K., Nemani, R., and Ban-Weiss, G.: Importance of carbon dioxide physiological forcing to future climate change, *PNAS*, 107, 9513–9518, <https://doi.org/10.1073/pnas.0913000107/-DCSupplemental>, 2010.
- Cao, R., Huang, H., Wu, G., Han, D., Jiang, Z., Di, K., and Hu, Z.: Spatiotemporal variations in the ratio of transpiration to evapotranspiration and its controlling factors across terrestrial biomes, *Agric. For. Meteorol.*, 321, <https://doi.org/10.1016/j.agrformet.2022.108984>, 2022.



- 695 Carneiro, R. G., Rykowska, Z., Borges, C. K., Stachlewska, I. S., and dos Santos, C. A. C.: Energy balance and  
Evapotranspiration response to environmental variables in the semi-arid Caatinga biome, *J. South Am. Earth Sci.*, 152,  
<https://doi.org/10.1016/j.jsames.2024.105319>, 2025.
- Chaney, N. W., Herman, J. D., Ek, M. B., and Wood, E. F.: Deriving global parameter estimates for the Noah land surface  
model using FLUXNET and machine learning, *J. Geophys. Res.*, 121, 13,218–13,235, <https://doi.org/10.1002/2016JD024821>,  
700 2016.
- Chatterjee, S., Swain, C. K., Nayak, A. K., Chatterjee, D., Bhattacharyya, P., Mahapatra, S. S., Debnath, M., Tripathi, R.,  
Guru, P. K., and Dhal, B.: Partitioning of eddy covariance-measured net ecosystem exchange of CO<sub>2</sub> in tropical lowland  
paddy, *Paddy and Water Environment*, 18, 623–636, <https://doi.org/10.1007/s10333-020-00806-7>, 2020.
- Chen, H., Wei, Y., and Huang, J. J.: Widespread increase in plant transpiration driven by global greening, *Glob. Planet.*  
705 *Change*, 235, <https://doi.org/10.1016/j.gloplacha.2024.104395>, 2024.
- Chen, Y., Ding, Z., Yu, P., Yang, H., Song, L., Fan, L., Han, X., Ma, M., and Tang, X.: Quantifying the variability in water  
use efficiency from the canopy to ecosystem scale across main croplands, *Agric. Water Manag.*, 262,  
<https://doi.org/10.1016/j.agwat.2021.107427>, 2022.
- Chen, Y., Tang, X., Yao, L., Zhao, Y., Li, G., Wu, C., Zhou, Y., and Sharma, A.: Management practices regulate the response  
710 of canopy and ecosystem water use efficiency in cropland ecosystems, *Field Crops Res.*, 304,  
<https://doi.org/10.1016/j.fcr.2023.109166>, 2023.
- Coenders-Gerrits, A. M. J., van der Ent, R. J., Bogaard, T. A., Wang-Erlandsson, L., Hrachowitz, M., and Savenije, H. H. G.:  
Uncertainties in transpiration estimates, <https://doi.org/10.1038/nature12926>, 2014.
- Cowan, I. R. and Farquhar, G. D.: Stomatal function in relation to leaf metabolism and environment: Stomatal function in the  
715 regulation of gas exchange, *Symp. Soc. Exp. Biol.*, 31, 471–505, 1977.
- Cui, N., Zheng, S., Jiang, S., Wang, M., Zhao, L., He, Z., Feng, Y., Wang, Y., Gong, D., Liu, C., and Qiu, R.:  
Evapotranspiration partitioning based on underlying conductance in a complex tree-grass orchard ecosystem in the humid area  
of southern China, *Agric. For. Meteorol.*, 344, <https://doi.org/10.1016/j.agrformet.2023.109796>, 2024.
- Czikowsky, M. J. and Fitzjarrald, D. R.: Detecting rainfall interception in an Amazonian rain forest with eddy flux  
720 measurements, *J. Hydrol. (Amst.)*, 377, 92–105, <https://doi.org/10.1016/j.jhydrol.2009.08.002>, 2009.
- D’Acunha, B., Dalmagro, H. J., Zanella de Arruda, P. H., Biudes, M. S., Lathuilière, M. J., Uribe, M., Couto, E. G., Brando,  
P. M., Vourlitis, G., and Johnson, M. S.: Changes in evapotranspiration, transpiration and evaporation across natural and  
managed landscapes in the Amazon, Cerrado and Pantanal biomes, *Agric. For. Meteorol.*, 346,  
<https://doi.org/10.1016/j.agrformet.2023.109875>, 2024.
- 725 Dawson, T. E., Burgess, S. S. O., Tu, K. P., Oliveira, R. S., Santiago, L. S., Fisher, J. B., Simonin, K. A., and Ambrose, A. R.:  
Nighttime transpiration in woody plants from contrasting ecosystems, *Tree Physiol.*, 27, 561–575,  
<https://doi.org/10.1093/treephys/27.4.561>, 2007.



- Day, M. E.: Influence of temperature and leaf-to-air vapor pressure deficit on net photosynthesis and stomatal conductance in red spruce (*Picea rubens*), *Tree Physiol.*, 20, 57–63, 2000.
- 730 Deb Burman, P. K., Chakraborty, S., El-Madany, T. S., Ramasubramanian, R., Gogoi, N., Gnanamoorthy, P., Murkute, C., Nagarajan, R., and Karipot, A.: A comparative study of ecohydrologies of a tropical mangrove and a broadleaf deciduous forest using eddy covariance measurement, *Meteorology and Atmospheric Physics*, 134, <https://doi.org/10.1007/s00703-021-00840-y>, 2022.
- Di, N., Xi, B., Clothier, B., Wang, Y., Li, G., and Jia, L.: Diurnal and nocturnal transpiration behaviors and their responses to groundwater-table fluctuations and meteorological factors of *Populus tomentosa* in the North China Plain, *For. Ecol. Manage.*, 448, 445–456, <https://doi.org/10.1016/j.foreco.2019.06.009>, 2019.
- 735 Dolman, A. J., Miralles, D. G., and de Jeu, R. A. M.: Fifty years since Monteith’s 1965 seminal paper: The emergence of global ecohydrology, <https://doi.org/10.1002/eco.1505>, 2014.
- Dorigo, W., Dietrich, S., Aires, F., Brocca, L., Carter, S., Cretaux, J. F., Dunkerley, D., Enomoto, H., Forsberg, R., Güntner, A., Heggin, M. I., Hollmann, R., Hurst, D. F., Johannessen, J. A., Kummerow, C., Lee, T., Luojus, K., Looser, U., Miralles, D. G., Pellet, V., Recknagel, T., Vargas, C. R., Schneider, U., Schoeneich, P., Schröder, M., Tapper, N., Vuglinsky, V., Wagner, W., Yu, L., Zappa, L., Zemp, M., and Aich, V.: Closing the water cycle from observations across scales where do we stand?, <https://doi.org/10.1175/BAMS-D-19-0316.1>, 1 October 2021.
- 740 Dukat, P., Ziemblińska, K., Räsänen, M., Vesala, T., Olejnik, J., and Urbaniak, M.: Scots pine responses to drought investigated with eddy covariance and sap flow methods, *Eur. J. For. Res.*, 142, 671–690, <https://doi.org/10.1007/s10342-023-01549-w>, 2023.
- Eichelmann, E., Mantoani, M. C., Chamberlain, S. D., Hemes, K. S., Oikawa, P. Y., Szutu, D., Valach, A., Verfaillie, J., and Baldocchi, D. D.: A novel approach to partitioning evapotranspiration into evaporation and transpiration in flooded ecosystems, *Glob. Chang. Biol.*, 28, 990–1007, <https://doi.org/10.1111/gcb.15974>, 2022.
- 750 El-Madany, T. S., Reichstein, M., Carrara, A., Martín, M. P., Moreno, G., Gonzalez-Cascon, R., Peñuelas, J., Ellsworth, D. S., Burchard-Levine, V., Hammer, T. W., Knauer, J., Kolle, O., Luo, Y., Pacheco-Labrador, J., Nelson, J. A., Perez-Priego, O., Rolo, V., Wutzler, T., and Migliavacca, M.: How Nitrogen and Phosphorus Availability Change Water Use Efficiency in a Mediterranean Savanna Ecosystem, *J. Geophys. Res. Biogeosci.*, 126, <https://doi.org/10.1029/2020JG006005>, 2021.
- Farquhar, G. D. and Sharkey, T. D.: Stomatal Conductance and Photosynthesis, *Annu. Rev. Plant Physiol.*, 33, 317–345, <https://doi.org/10.1146/annurev.pp.33.060182.001533>, 1982.
- 755 Fatichi, S. and Pappas, C.: Constrained variability of modeled T:ET ratio across biomes, *Geophys. Res. Lett.*, 44, 6795–6803, <https://doi.org/10.1002/2017GL074041>, 2017.
- Ferrara, R. M., Azzolini, A., Ciurlia, A., De Carolis, G., Mastrangelo, M., Minorenti, V., Montagni, A., Piarulli, M., Ruggieri, S., Vitti, C., Martinelli, N., and Rana, G.: Carbon and Water Balances in a Watermelon Crop Mulched with Biodegradable Films in Mediterranean Conditions at Extended Growth Season Scale, *Atmosphere (Basel)*, 15, <https://doi.org/10.3390/atmos15080945>, 2024.
- 760



- Fischer, S., Queck, R., Bernhofer, C., and Mauder, M.: Quantifying evaporation of intercepted rainfall: a hybrid correction approach for eddy-covariance measurements, *Hydrol. Earth Syst. Sci.*, 30, 965–984, <https://doi.org/10.5194/hess-30-965-2026>, 2026.
- 765 Fisher, J. B., Melton, F., Middleton, E., Hain, C., Anderson, M., Allen, R., McCabe, M. F., Hook, S., Baldocchi, D., Townsend, P. A., Kilic, A., Tu, K., Miralles, D. D., Perret, J., Lagouarde, J. P., Waliser, D., Purdy, A. J., French, A., Schimel, D., Famiglietti, J. S., Stephens, G., and Wood, E. F.: The future of evapotranspiration: Global requirements for ecosystem functioning, carbon and climate feedbacks, agricultural management, and water resources, <https://doi.org/10.1002/2016WR020175>, 1 April 2017.
- 770 Friend, A. D., Arneeth, A., Kiang, N. Y., Lomas, M., Ogée, J., Rödenbeck, C., Running, S. W., Santaren, J. D., Sitch, S., Viovy, N., Ian Woodward, F., and Zaehle, S.: FLUXNET and modelling the global carbon cycle, *Glob. Chang. Biol.*, 13, 610–633, <https://doi.org/10.1111/j.1365-2486.2006.01223.x>, 2007.
- Gan, G. and Liu, Y.: Inferring transpiration from evapotranspiration: A transpiration indicator using the Priestley-Taylor coefficient of wet environment, *Ecol. Indic.*, 110, <https://doi.org/10.1016/j.ecolind.2019.105853>, 2020.
- 775 Gao, H., Cai, Q., Shi, X., Shan, S., and Zhuang, H.: Assessment of irrigation efficiency for arid-zone spring wheat production under flood irrigation, *Irrig. Sci.*, <https://doi.org/10.1007/s00271-024-00946-2>, 2024.
- Gao, H., Cai, Q., Shi, X., Shan, S., and Zhuang, H.: Assessment of irrigation efficiency for arid-zone spring wheat production under flood irrigation, *Irrig. Sci.*, 43, 347–362, <https://doi.org/10.1007/s00271-024-00946-2>, 2025.
- Gedney, N., Cox, P. M., Betts, R. A., Boucher, O., Huntingford, C., and Stott, P. A.: Detection of a direct carbon dioxide effect in continental river runoff records, *Nature*, 439, 835–838, <https://doi.org/10.1038/nature04504>, 2006.
- 780 Gerken, T., Bromley, G. T., and Stoy, P. C.: Surface moistening trends in the Northern North American great plains increase the likelihood of convective initiation, *J. Hydrometeorol.*, 19, 227–244, <https://doi.org/10.1175/JHM-D-17-0117.1>, 2018.
- Gerrits, A. M. J., Pfister, L., and Savenije, H. H. G.: Spatial and temporal variability of canopy and forest floor interception in a beech forest, *Hydrol. Process.*, 24, 3011–3025, <https://doi.org/10.1002/hyp.7712>, 2010.
- 785 Gnanamoorthy, P., Zhao, J., Chakraborty, A., Burman, P. K. D., Chen, Y., Jiao, L., Zhang, J., Liu, Y., Sivaraj, S., Zhang, Y., and Song, Q.: Asynchronous recovery of evaporation and transpiration following extreme snow damage in a subtropical forest, *J. Hydrol. Reg. Stud.*, 55, <https://doi.org/10.1016/j.ejrh.2024.101947>, 2024.
- Good, S. P., Soderberg, K., Guan, K., King, E. G., Scanlon, T. M., and Caylor, K. K.:  $\delta^2\text{H}$  isotopic flux partitioning of evapotranspiration over a grass field following a water pulse and subsequent dry down, *Water Resour. Res.*, 50, 1410–1432, <https://doi.org/10.1002/2013WR014333>, 2014.
- 790 Good, S. P., Noone, D., Kurita, N., Benetti, M., and Bowen, G. J.: D/H isotope ratios in the global hydrologic cycle, *Geophys. Res. Lett.*, 42, 5042–5050, <https://doi.org/10.1002/2015GL064117>, 2015.
- Griffis, T. J.: Tracing the flow of carbon dioxide and water vapor between the biosphere and atmosphere: A review of optical isotope techniques and their application, <https://doi.org/10.1016/j.agrformet.2013.02.009>, 15 June 2013.



- 795 Grossiord, C., Buckley, T. N., Cernusak, L. A., Novick, K. A., Poulter, B., Siegwolf, R. T. W., Sperry, J. S., and McDowell, N. G.: Plant responses to rising vapor pressure deficit, *New Phytologist*, 226, 1550–1566, <https://doi.org/10.1111/nph.16485>, 2020.
- De Haan, K., Khomik, M., Green, A., Helgason, W., Macrae, M. L., Kompanizare, M., and Petrone, R. M.: Assessment of different water use efficiency calculations for dominant forage crops in the great lakes basin, *Agriculture (Switzerland)*, 11, 800 <https://doi.org/10.3390/agriculture11080739>, 2021.
- Han, D., Wang, G., Liu, T., Xue, B. L., Kuczera, G., and Xu, X.: Hydroclimatic response of evapotranspiration partitioning to prolonged droughts in semiarid grassland, *J. Hydrol. (Amst.)*, 563, 766–777, <https://doi.org/10.1016/j.jhydrol.2018.06.048>, 2018.
- Hao, S., Jia, X., Zhao, H., Li, X., Mu, Y., Zha, T., Liu, P., and Bourque, C. P. A.: Evapotranspiration and its partitioning during and following a mountain pine beetle infestation of a lodgepole pine stand in the interior of British Columbia, Canada, *Frontiers in Forests and Global Change*, 7, <https://doi.org/10.3389/ffgc.2024.1352853>, 2024.
- Hatfield, J. L. and Dold, C.: Water-use efficiency: Advances and challenges in a changing climate, <https://doi.org/10.3389/fpls.2019.00103>, 19 February 2019.
- Hu, H., Chen, L., Liu, H., Khan, M. Y. A., Tie, Q., Zhang, X., and Tian, F.: Comparison of the vegetation effect on ET 810 partitioning based on eddy covariance method at five different sites of Northern China, *Remote Sens. (Basel.)*, 10, <https://doi.org/10.3390/rs10111755>, 2018.
- Hu, X. and Lei, H.: Evapotranspiration partitioning and its interannual variability over a winter wheat-summer maize rotation system in the North China Plain, *Agric. For. Meteorol.*, 310, <https://doi.org/10.1016/j.agrformet.2021.108635>, 2021.
- Jasechko, S., Sharp, Z. D., Gibson, J. J., Birks, S. J., Yi, Y., and Fawcett, P. J.: Terrestrial water fluxes dominated by 815 transpiration, *Nature*, 496, 347–350, <https://doi.org/10.1038/nature11983>, 2013.
- Jiang, S., Liang, C., Cui, N., Zhao, L., Liu, C., Feng, Y., Hu, X., Gong, D., and Zou, Q.: Water use efficiency and its drivers in four typical agroecosystems based on flux tower measurements, *Agric. For. Meteorol.*, 295, <https://doi.org/10.1016/j.agrformet.2020.108200>, 2020.
- Jin, J., Yan, T., Wang, H., Ma, X., He, M., Wang, Y., Wang, W., Guo, F., Cai, Y., Zhu, Q., and Wu, J.: Improved modeling of 820 canopy transpiration for temperate forests by incorporating a LAI-based dynamic parametrization scheme of stomatal slope, *Agric. For. Meteorol.*, 326, <https://doi.org/10.1016/j.agrformet.2022.109157>, 2022.
- Jocher, G., Marshall, J., Nilsson, M. B., Linder, S., De Simon, G., Hörnlund, T., Lundmark, T., Näsholm, T., Ottosson Löfvenius, M., Tarvainen, L., Wallin, G., and Peichl, M.: Impact of Canopy Decoupling and Subcanopy Advection on the Annual Carbon Balance of a Boreal Scots Pine Forest as Derived From Eddy Covariance, *J. Geophys. Res. Biogeosci.*, 123, 825 303–325, <https://doi.org/10.1002/2017JG003988>, 2018.
- Jung, M., Reichstein, M., Ciais, P., Seneviratne, S. I., Sheffield, J., Goulden, M. L., Bonan, G., Cescatti, A., Chen, J., De Jeu, R., Dolman, A. J., Eugster, W., Gerten, D., Gianelle, D., Gobron, N., Heinke, J., Kimball, J., Law, B. E., Montagnani, L., Mu, Q., Mueller, B., Oleson, K., Papale, D., Richardson, A. D., Rouspard, O., Running, S., Tomelleri, E., Viovy, N., Weber, U.,



- Williams, C., Wood, E., Zaehle, S., and Zhang, K.: Recent decline in the global land evapotranspiration trend due to limited  
830 moisture supply, *Nature*, 467, 951–954, <https://doi.org/10.1038/nature09396>, 2010.
- Jung, M., Koirala, S., Weber, U., Ichii, K., Gans, F., Camps-Valls, G., Papale, D., Schwalm, C., Tramontana, G., and Reichstein, M.: The FLUXCOM ensemble of global land-atmosphere energy fluxes, *Sci. Data*, 6, <https://doi.org/10.1038/s41597-019-0076-8>, 2019.
- Katul, G. G., Palmroth, S., and Oren, R.: Leaf stomatal responses to vapour pressure deficit under current and CO<sub>2</sub>-enriched  
835 atmosphere explained by the economics of gas exchange, *Plant Cell Environ.*, 32, 968–979, <https://doi.org/10.1111/j.1365-3040.2009.01977.x>, 2009.
- Katul, G. G., Oren, R., Manzoni, S., Higgins, C., and Parlange, M. B.: Evapotranspiration: A process driving mass transport and energy exchange in the soil-plant-atmosphere-climate system, <https://doi.org/10.1029/2011RG000366>, 1 September 2012.
- Kibler, C. L., Trugman, A. T., Roberts, D. A., Still, C. J., Scott, R. L., Caylor, K. K., Stella, J. C., and Singer, M. B.:  
840 Evapotranspiration regulates leaf temperature and respiration in dryland vegetation, *Agric. For. Meteorol.*, 339, <https://doi.org/10.1016/j.agrformet.2023.109560>, 2023.
- Kim, S. H., Sicher, R. C., Bae, H., Gitz, D. C., Baker, J. T., Timlin, D. J., and Reddy, V. R.: Canopy photosynthesis, evapotranspiration, leaf nitrogen, and transcription profiles of maize in response to CO<sub>2</sub> enrichment, *Glob. Chang. Biol.*, 12, 588–600, <https://doi.org/10.1111/j.1365-2486.2006.01110.x>, 2006.
- 845 Klosterhalfen, A., Moene, A. F., Schmidt, M., Scanlon, T. M., Vereecken, H., and Graf, A.: Sensitivity analysis of a source partitioning method for H<sub>2</sub>O and CO<sub>2</sub> fluxes based on high frequency eddy covariance data: Findings from field data and large eddy simulations, *Agric. For. Meteorol.*, 265, 152–170, <https://doi.org/10.1016/j.agrformet.2018.11.003>, 2019a.
- Klosterhalfen, A., Graf, A., Brüggemann, N., Drüe, C., Esser, O., González-Dugo, M. P., Heinemann, G., Jacobs, C. M. J., Mauder, M., Moene, A. F., Ney, P., Pütz, T., Rebmann, C., Rodríguez, M. R., Scanlon, T. M., Schmidt, M., Steinbrecher, R.,  
850 Thomas, C. K., Valler, V., Zeeman, M. J., and Vereecken, H.: Source partitioning of H<sub>2</sub>O and CO<sub>2</sub> fluxes based on high-frequency eddy covariance data: A comparison between study sites, *Biogeosciences*, 16, 1111–1132, <https://doi.org/10.5194/bg-16-1111-2019>, 2019b.
- Knowles, J. F., Bjarke, N. R., Badger, A. M., Berkelhammer, M., Biederman, J. A., Blanken, P. D., Bretfeld, M., Burns, S. P., Ewers, B. E., Frank, J. M., Hicke, J. A., Lestak, L., Livneh, B., Reed, D. E., Scott, R. L., and Molotch, N. P.: Bark beetle  
855 impacts on forest evapotranspiration and its partitioning, *Science of the Total Environment*, 880, <https://doi.org/10.1016/j.scitotenv.2023.163260>, 2023.
- Kool, D., Agam, N., Lazarovitch, N., Heitman, J. L., Sauer, T. J., and Ben-Gal, A.: A review of approaches for evapotranspiration partitioning, <https://doi.org/10.1016/j.agrformet.2013.09.003>, 15 January 2014.
- Kurc, S. A. and Small, E. E.: Soil moisture variations and ecosystem-scale fluxes of water and carbon in semiarid grassland  
860 and shrubland, *Water Resour. Res.*, 43, <https://doi.org/10.1029/2006WR005011>, 2007.
- Kustas, W. P., Anderson, M. C., Alfieri, J. G., Knipppper, K., Torres-Rua, A., Parry, C. K., Nieto, H., Agam, N., White, W. A., Gao, F., McKee, L., Prueger, J. H., Hipppps, L. E., Los, S., Alsina, M. M., Sanchez, L., Sams, B., Dokoozlian, N., McKee,



- M., Jones, S., Yang, Y., Wilson, T. G., Lei, F., McElrone, A., Heitman, J. L., Howard, A. M., Post, K., Melton, F., and Hain, C.: The grape remote sensing atmospheric profile and evapotranspiration experiment, *Bull. Am. Meteorol. Soc.*, 99, 1791–1812, <https://doi.org/10.1175/BAMS-D-16-0244.1>, 2018.
- 865 Kustas, W. P., Agam, N., Alfieri, J. G., McKee, L. G., Prueger, J. H., Hipps, L. E., Howard, A. M., and Heitman, J. L.: Below canopy radiation divergence in a vineyard: implications on interrow surface energy balance, *Irrig. Sci.*, 37, 227–237, <https://doi.org/10.1007/s00271-018-0601-0>, 2019a.
- Kustas, W. P., Alfieri, J. G., Nieto, H., Wilson, T. G., Gao, F., and Anderson, M. C.: Utility of the two-source energy balance (TSEB) model in vine and interrow flux partitioning over the growing season, *Irrig. Sci.*, 37, 375–388, <https://doi.org/10.1007/s00271-018-0586-8>, 2019b.
- Lasslop, G., Reichstein, M., Papale, D., Richardson, A. D., Arneeth, A., Barr, A., Stoy, P., and Wohlfahrt, G.: Separation of net ecosystem exchange into assimilation and respiration using a light response curve approach: critical issues and global evaluation, *Glob. Chang. Biol.*, 16, 187–208, <https://doi.org/10.1111/j.1365-2486.2009.02041.x>, 2010.
- 875 Li, C., Han, J., Liu, Z., Tu, Z., and Yang, H.: A harmonized global gridded transpiration product based on collocation analysis, *Sci. Data*, 11, <https://doi.org/10.1038/s41597-024-03425-7>, 2024a.
- Li, H., Chen, H., and Huang, J. J.: Partitioning urban forest evapotranspiration based on integrating eddy covariance of water vapor and carbon dioxide fluxes, *Science of the Total Environment*, 935, <https://doi.org/10.1016/j.scitotenv.2024.173201>, 2024b.
- 880 Li, J., Yuan, J., Liu, D., Zhao, X., Dong, Y., Zheng, H., Li, Y., and Ding, W.: Inter- and intra-annual variability and climatic responses of ecosystem water use efficiency in a cool-temperate freshwater wetland, *Ecol. Indic.*, 167, <https://doi.org/10.1016/j.ecolind.2024.112663>, 2024c.
- Li, M., Shao, W., Su, Y., Coenders-Gerrits, M., and Jarsjö, J.: Evidence of field-scale shifts in transpiration dynamics following bark beetle infestation: Stomatal conductance responses, *Hydrol. Process.*, 38, <https://doi.org/10.1002/hyp.15162>, 2024d.
- 885 Li, X., Gentine, P., Lin, C., Zhou, S., Sun, Z., Zheng, Y., Liu, J., and Zheng, C.: A simple and objective method to partition evapotranspiration into transpiration and evaporation at eddy-covariance sites, *Agric. For. Meteorol.*, 265, 171–182, <https://doi.org/10.1016/j.agrformet.2018.11.017>, 2019.
- Li, X., Black, T. A., Zha, T., Jassal, R. S., Nestic, Z., Lee, S. C., Bourque, C. P. A., Hao, S., Jin, C., Liu, P., Jia, X., and Tian, Y.: Long-term trend and interannual variation in evapotranspiration of a young temperate Douglas-fir stand over 2002–2022 reveals the impacts of climate change, *Plant Cell Environ.*, <https://doi.org/10.1111/pce.15000>, 2024e.
- 890 Lian, X., Piao, S., Huntingford, C., Li, Y., Zeng, Z., Wang, X., Ciais, P., McVicar, T. R., Peng, S., Ottlé, C., Yang, H., Yang, Y., Zhang, Y., and Wang, T.: Partitioning global land evapotranspiration using CMIP5 models constrained by observations, *Nat. Clim. Chang.*, 8, 640–646, <https://doi.org/10.1038/s41558-018-0207-9>, 2018.
- Lian, X., Zhao, W., and Gentine, P.: Recent global decline in rainfall interception loss due to altered rainfall regimes, *Nat. Commun.*, 13, <https://doi.org/10.1038/s41467-022-35414-y>, 2022.
- 895



- Lin, C., Gentine, P., Huang, Y., Guan, K., Kimm, H., and Zhou, S.: Diel ecosystem conductance response to vapor pressure deficit is suboptimal and independent of soil moisture, *Agric. For. Meteorol.*, 250–251, 24–34, <https://doi.org/10.1016/j.agrformet.2017.12.078>, 2018.
- Liu, B., Hou, J., Ge, H., Liu, M., Shi, L., Li, C., and Cui, Y.: Comparison of Evapotranspiration Partitioning and Dual Crop Coefficients of Direct-Seeded and Transplanted Rice in the Poyang Lake Basin, China, *Agronomy*, 13, 900 <https://doi.org/10.3390/agronomy13051218>, 2023.
- Liu, M., Tang, R., Li, Z. L., Duan, S., Gao, M., Xu, Z., and Song, L.: Separating soil evaporation from vegetation transpiration by remotely sensed one-phase and two-phase trapezoids, *Agric. For. Meteorol.*, 327, <https://doi.org/10.1016/j.agrformet.2022.109215>, 2022a.
- 905 Liu, P., Zha, T., Jia, X., Tian, Y., Hao, S., and Li, X.: Divergent responses of canopy and ecosystem water use efficiency to environmental conditions over a decade in a shrubland ecosystem dominated by *Artemisia ordosica*, *Agric. For. Meteorol.*, 368, <https://doi.org/10.1016/j.agrformet.2025.110551>, 2025.
- Liu, Y. and Qiao, C.: Partitioning Evapotranspiration in a Cotton Field under Mulched Drip Irrigation Based on the Water-Carbon Fluxes Coupling in an Arid Region in Northwestern China, *Agriculture (Switzerland)*, 13, 910 <https://doi.org/10.3390/agriculture13061219>, 2023.
- Liu, Y., Zhang, Y., Shan, N., Zhang, Z., and Wei, Z.: Global assessment of partitioning transpiration from evapotranspiration based on satellite solar-induced chlorophyll fluorescence data, *J. Hydrol. (Amst.)*, 612, <https://doi.org/10.1016/j.jhydrol.2022.128044>, 2022b.
- Liu, Y., Liu, H., Li, F., Du, Q., Xu, L., and Li, Y.: Interannual Variations of Water and Carbon Dioxide Fluxes over a Semiarid 915 Alpine Steppe on the Tibetan Plateau, *Advances in Meteorology*, 2022, <https://doi.org/10.1155/2022/7368882>, 2022c.
- López, J., Way, D. A., and Sadok, W.: Systemic effects of rising atmospheric vapor pressure deficit on plant physiology and productivity, <https://doi.org/10.1111/gcb.15548>, 1 May 2021a.
- López, J. R., Schoppach, R., and Sadok, W.: Harnessing nighttime transpiration dynamics for drought tolerance in grasses, *Plant Signal. Behav.*, 16, 1875646, <https://doi.org/10.1080/15592324.2021.1875646>, 2021b.
- 920 Lowry, A. L., McGowan, H. A., and Gray, M. A.: Multi-year carbon and water exchanges over contrasting ecosystems on a sub-tropical sand island, *Agric. For. Meteorol.*, 304–305, <https://doi.org/10.1016/j.agrformet.2021.108404>, 2021.
- Lu, L., Zhang, D., Zhang, J., Zhang, J., Zhang, S., Bai, Y., and Yang, S.: Ecosystem Evapotranspiration Partitioning and Its Spatial–Temporal Variation Based on Eddy Covariance Observation and Machine Learning Method, *Remote Sens. (Basel)*, 15, <https://doi.org/10.3390/rs15194831>, 2023.
- 925 Ma, S., Eichelmann, E., Wolf, S., Rey-Sanchez, C., and Baldocchi, D. D.: Transpiration and evaporation in a Californian oak-grass savanna: Field measurements and partitioning model results, *Agric. For. Meteorol.*, 295, <https://doi.org/10.1016/j.agrformet.2020.108204>, 2020.



- MacBean, N., Scott, R. L., Biederman, J. A., Ottlé, C., Vuichard, N., Ducharne, A., Kolb, T., Dore, S., Litvak, M., and Moore, D. J. P.: Testing water fluxes and storage from two hydrology configurations within the ORCHIDEE land surface model across  
930 US semi-arid sites, *Hydrol. Earth Syst. Sci.*, 24, 5203–5230, <https://doi.org/10.5194/hess-24-5203-2020>, 2020.
- Maes, W. H., Pagán, B. R., Martens, B., Gentine, P., Guanter, L., Steppe, K., Verhoest, N. E. C., Dorigo, W., Li, X., Xiao, J., and Miralles, D. G.: Sun-induced fluorescence closely linked to ecosystem transpiration as evidenced by satellite data and radiative transfer models, *Remote Sens. Environ.*, 249, <https://doi.org/10.1016/j.rse.2020.112030>, 2020.
- Maxwell, R. M. and Condon, L. E.: Connections between groundwater flow and transpiration partitioning, *Science* (1979)., 935 353, 377–380, <https://doi.org/10.1126/science.aaf7891>, 2016.
- Medlyn, B. E., De Kauwe, M. G., Lin, Y. S., Knauer, J., Duursma, R. A., Williams, C. A., Arneeth, A., Clement, R., Isaac, P., Limousin, J. M., Linderson, M. L., Meir, P., Martin-Stpaul, N., and Wingate, L.: How do leaf and ecosystem measures of water-use efficiency compare?, *New Phytologist*, 216, 758–770, <https://doi.org/10.1111/nph.14626>, 2017.
- Miralles, D. G., Gash, J. H., Holmes, T. R. H., De Jeu, R. A. M., and Dolman, A. J.: Global canopy interception from satellite  
940 observations, *Journal of Geophysical Research Atmospheres*, 115, <https://doi.org/10.1029/2009JD013530>, 2010.
- Miralles, D. G., De Jeu, R. A. M., Gash, J. H., Holmes, T. R. H., and Dolman, A. J.: Magnitude and variability of land evaporation and its components at the global scale, *Hydrol. Earth Syst. Sci.*, 15, 967–981, <https://doi.org/10.5194/hess-15-967-2011>, 2011.
- Misson, L., Baldocchi, D. D., Black, T. A., Blanken, P. D., Brunet, Y., Curiel Yuste, J., Dorsey, J. R., Falk, M., Granier, A.,  
945 Irvine, M. R., Jarosz, N., Lamaud, E., Launiainen, S., Law, B. E., Longdoz, B., Loustau, D., McKay, M., Paw U, K. T., Vesala, T., Vickers, D., Wilson, K. B., and Goldstein, A. H.: Partitioning forest carbon fluxes with overstory and understory eddy-covariance measurements: A synthesis based on FLUXNET data, *Agric. For. Meteorol.*, 144, 14–31, <https://doi.org/10.1016/j.agrformet.2007.01.006>, 2007.
- Monteith, J. L.: Evaporation and environment, *Symp. Soc. Exp. Biol.*, 19, 205–234, 1965.
- 950 Morison, J. I. L. and Gifford, R. M.: Stomatal Sensitivity to Carbon Dioxide and Humidity, *Plant Physiol.*, 71, 789–796, <https://doi.org/10.1104/pp.71.4.789>, 1983.
- Nelson, J. A., Carvalhais, N., Cuntz, M., Delpierre, N., Knauer, J., Ogée, J., Migliavacca, M., Reichstein, M., and Jung, M.: Coupling Water and Carbon Fluxes to Constrain Estimates of Transpiration: The TEA Algorithm, *J. Geophys. Res. Biogeosci.*, 123, 3617–3632, <https://doi.org/10.1029/2018JG004727>, 2018.
- 955 Nelson, J. A., Pérez-Priego, O., Zhou, S., Poyatos, R., Zhang, Y., Blanken, P. D., Gimeno, T. E., Wohlfahrt, G., Desai, A. R., Gioli, B., Limousin, J. M., Bonal, D., Paul-Limoges, E., Scott, R. L., Varlagin, A., Fuchs, K., Montagnani, L., Wolf, S., Delpierre, N., Berveiller, D., Gharun, M., Belelli Marchesini, L., Gianelle, D., Šigut, L., Mammarella, I., Siebicke, L., Andrew Black, T., Knohl, A., Hörtnagl, L., Magliulo, V., Besnard, S., Weber, U., Carvalhais, N., Migliavacca, M., Reichstein, M., and Jung, M.: Ecosystem transpiration and evaporation: Insights from three water flux partitioning methods across FLUXNET  
960 sites, *Glob. Chang. Biol.*, 26, 6916–6930, <https://doi.org/10.1111/gcb.15314>, 2020.



- Nie, C., Huang, Y., Zhang, S., Yang, Y., Zhou, S., Lin, C., and Wang, G.: Effects of soil water content on forest ecosystem water use efficiency through changes in transpiration/evapotranspiration ratio, *Agric. For. Meteorol.*, 308–309, <https://doi.org/10.1016/j.agrformet.2021.108605>, 2021.
- 965 Nogueira, M., Boussetta, S., Balsamo, G., Albergel, C., Trigo, I. F., Johannsen, F., Miralles, D. G., and Dutra, E.: Upgrading Land-Cover and Vegetation Seasonality in the ECMWF Coupled System: Verification With FLUXNET Sites, METEOSAT Satellite Land Surface Temperatures, and ERA5 Atmospheric Reanalysis, *Journal of Geophysical Research: Atmospheres*, 126, <https://doi.org/10.1029/2020JD034163>, 2021.
- Novick, K. A., Ficklin, D. L., Stoy, P. C., Williams, C. A., Bohrer, G., Oishi, A. C., Papuga, S. A., Blanken, P. D., Noormets, A., Sulman, B. N., Scott, R. L., Wang, L., and Phillips, R. P.: The increasing importance of atmospheric demand for ecosystem water and carbon fluxes, *Nat. Clim. Chang.*, 6, 1023–1027, <https://doi.org/10.1038/nclimate3114>, 2016.
- 970 Ocheltree, T. W., Nippert, J. B., and Prasad, P. V. V.: Stomatal responses to changes in vapor pressure deficit reflect tissue-specific differences in hydraulic conductance, *Plant Cell Environ.*, 37, 132–139, <https://doi.org/10.1111/pce.12137>, 2014.
- Ohkubo, S., Hirano, T., and Kusin, K.: Influence of disturbance on transpiration and evaporation in tropical peat swamp forests, *J. Hydrol. (Amst.)*, 620, <https://doi.org/10.1016/j.jhydrol.2023.129523>, 2023.
- 975 Oishi, A. C., Oren, R., and Stoy, P. C.: Estimating components of forest evapotranspiration: A footprint approach for scaling sap flux measurements, *Agric. For. Meteorol.*, 148, 1719–1732, <https://doi.org/10.1016/j.agrformet.2008.06.013>, 2008.
- Oki, T. and Kanae, S.: *Global Hydrological Cycles and World Water Resources*, 2006.
- Paciolla, N., Corbari, C., Kustas, W. P., Nieto, H., Alfieri, J. G., Zahn, E., Gao, F., Prueger, J. H., Alsina, M. M., Hipps, L. E., McKee, L. G., McElrone, A. J., and Bambach, N.: Two-source energy balance schemes exploiting land surface temperature and soil moisture for continuous vineyard water use estimation, *Irrig. Sci.*, 43, 731–753, <https://doi.org/10.1007/s00271-024-00991-x>, 2025.
- 980 Pagán, B. R., Maes, W. H., Gentine, P., Martens, B., and Miralles, D. G.: Exploring the potential of satellite solar-induced fluorescence to constrain global transpiration estimates, *Remote Sens. (Basel)*, 11, <https://doi.org/10.3390/rs11040413>, 2019.
- Palatella, L., Rana, G., and Vitale, D.: Towards a Flux-Partitioning Procedure Based on the Direct Use of High-Frequency Eddy-Covariance Data, *Boundary. Layer. Meteorol.*, 153, 327–337, <https://doi.org/10.1007/s10546-014-9947-x>, 2014.
- 985 Paschalis, A., Fatichi, S., Pappas, C., and Or, D.: Covariation of vegetation and climate constrains present and future T/ET variability, *Environmental Research Letters*, 13, <https://doi.org/10.1088/1748-9326/aae267>, 2018.
- Paul-Limoges, E., Wolf, S., Eugster, W., Hörtnagl, L., and Buchmann, N.: Below-canopy contributions to ecosystem CO<sub>2</sub> fluxes in a temperate mixed forest in Switzerland, *Agric. For. Meteorol.*, 247, 582–596, <https://doi.org/10.1016/j.agrformet.2017.08.011>, 2017.
- 990 Paul-Limoges, E., Revill, A., Maier, R., Buchmann, N., and Damm, A.: Insights for the Partitioning of Ecosystem Evaporation and Transpiration in Short-Statured Croplands, *J. Geophys. Res. Biogeosci.*, 127, <https://doi.org/10.1029/2021JG006760>, 2022.



- Peddinti, S. R. and Kambhammettu, B. P.: Dynamics of crop coefficients for citrus orchards of central India using water balance and eddy covariance flux partition techniques, *Agric. Water Manag.*, 212, 68–77, <https://doi.org/10.1016/j.agwat.2018.08.027>, 2019.
- Peng, X., Liu, X., Wang, Y., and Cai, H.: Evapotranspiration Partitioning and Estimation Based on Crop Coefficients of Winter Wheat Cropland in the Guanzhong Plain, China, *Agronomy*, 13, <https://doi.org/10.3390/agronomy13122982>, 2023.
- Penman, H. L.: Natural evaporation from open water, bare soil and grass, *Proc. R. Soc. Lond. A Math. Phys. Sci.*, 193, 120–145, <https://doi.org/10.1098/rspa.1948.0037>, 1948.
- Perez-Priego, O., Katul, G., Reichstein, M., El-Madany, T. S., Ahrens, B., Carrara, A., Scanlon, T. M., and Migliavacca, M.: Partitioning Eddy Covariance Water Flux Components Using Physiological and Micrometeorological Approaches, *J. Geophys. Res. Biogeosci.*, 123, 3353–3370, <https://doi.org/10.1029/2018JG004637>, 2018.
- Perez-Quezada, J. F., Trejo, D., Lopatin, J., Aguilera, D., Osborne, B., Galleguillos, M., Zattera, L., Celis-Diez, J. L., and Armesto, J. J.: Comparison of carbon and water fluxes and the drivers of ecosystem water use efficiency in a temperate rainforest and a peatland in southern South America, *Biogeosciences*, 21, 1371–1389, <https://doi.org/10.5194/bg-21-1371-2024>, 2024.
- Poyatos, R., Granda, V., Molowny-Horas, R., Mencuccini, M., Steppe, K., and Martínez-Vilalta, J.: SAPFLUXNET: Towards a global database of sap flow measurements, *Tree Physiol.*, 36, 1449–1455, <https://doi.org/10.1093/treephys/tpw110>, 2016.
- Raghav, P., Wagle, P., Kumar, M., Banerjee, T., and Neel, J. P. S.: Vegetation Index-Based Partitioning of Evapotranspiration Is Deficient in Grazed Systems, *Water Resour. Res.*, 58, <https://doi.org/10.1029/2022WR032067>, 2022.
- Rana, G., Palatella, L., Scanlon, T. M., Martinelli, N., and Ferrara, R. M.: CO<sub>2</sub> and H<sub>2</sub>O flux partitioning in a Mediterranean cropping system, *Agric. For. Meteorol.*, 260–261, 118–130, <https://doi.org/10.1016/j.agrformet.2018.06.007>, 2018.
- Rana, G., De Lorenzi, F., Palatella, L., Martinelli, N., and Ferrara, R. M.: Field scale recalibration of the sap flow thermal dissipation method in a Mediterranean vineyard, *Agric. For. Meteorol.*, 269–270, 169–179, <https://doi.org/10.1016/j.agrformet.2019.02.018>, 2019.
- Ranjbar, S., Zahn, E., Losos, D., Hoffman, S., Shrestha, O., Bou-Zeid, E., and Stoy, P. C.: Partitioning Ecosystem Water Fluxes Into Transpiration, Surface Evaporation, and Canopy-Intercepted Evaporation Using Knowledge-Guided Machine Learning at NEON Sites, *J. Geophys. Res. Biogeosci.*, 131, <https://doi.org/10.1029/2025JG009478>, 2026.
- Räsänen, M., Aurela, M., Vakkari, V., Beukes, J. P., Tuovinen, J. P., Van Zyl, P. G., Josipovic, M., Siebert, S. J., Laurila, T., Kulmala, M., Laakso, L., Rinne, J., Oren, R., and Katul, G.: The effect of rainfall amount and timing on annual transpiration in a grazed savanna grassland, *Hydrol. Earth Syst. Sci.*, 26, 5773–5791, <https://doi.org/10.5194/hess-26-5773-2022>, 2022.
- Reavis, C. W., Reba, M. L., and Runkle, B. R. K.: The effects of alternate wetting and drying irrigation on water use efficiency in Mid-South rice, *Agric. For. Meteorol.*, 353, <https://doi.org/10.1016/j.agrformet.2024.110069>, 2024.
- Reich, E. G., Samuels-Crow, K., Bradford, J. B., Litvak, M., Schlaepfer, D. R., and Ogle, K.: A Semi-Mechanistic Model for Partitioning Evapotranspiration Reveals Transpiration Dominates the Water Flux in Drylands, *J. Geophys. Res. Biogeosci.*, 129, <https://doi.org/10.1029/2023JG007914>, 2024.



- Reichstein, M., Falge, E., Baldocchi, D., Papale, D., Aubinet, M., Berbigier, P., Bernhofer, C., Buchmann, N., Gilmanov, T., Granier, A., Grünwald, T., Havránková, K., Ilvesniemi, H., Janous, D., Knohl, A., Laurila, T., Lohila, A., Loustau, D.,  
1030 Matteucci, G., Meyers, T., Miglietta, F., Ourcival, J. M., Pumpanen, J., Rambal, S., Rotenberg, E., Sanz, M., Tenhunen, J.,  
Seufert, G., Vaccari, F., Vesala, T., Yakir, D., and Valentini, R.: On the separation of net ecosystem exchange into assimilation  
and ecosystem respiration: Review and improved algorithm, <https://doi.org/10.1111/j.1365-2486.2005.001002.x>, September  
2005.
- Restrepo-Coupe, N., O'Donnell Christoffersen, B., Longo, M., Alves, L. F., Campos, K. S., da Araujo, A. C., de Oliveira, R.  
1035 C., Prohaska, N., da Silva, R., Tapajos, R., Wiedemann, K. T., Wofsy, S. C., and Saleska, S. R.: Asymmetric response of  
Amazon forest water and energy fluxes to wet and dry hydrological extremes reveals onset of a local drought-induced tipping  
point, *Glob. Chang. Biol.*, 29, 6077–6092, <https://doi.org/10.1111/gcb.16933>, 2023.
- da Rocha, A. E. Q., Santos, E. A., and Patrignani, A.: Partitioning evapotranspiration in a tallgrass prairie using  
micrometeorological and water use efficiency approaches under contrasting rainfall regimes, *J. Hydrol. (Amst.)*, 608,  
1040 <https://doi.org/10.1016/j.jhydrol.2022.127624>, 2022.
- da Rocha, A. E. Q., Santos, E. A., and Owensby, C.: Partitioning evapotranspiration and carbon flux in ungrazed and grazed  
tallgrass prairie, *Agric. Ecosyst. Environ.*, 343, <https://doi.org/10.1016/j.agee.2022.108285>, 2023.
- Salemi, L. F., Groppo, J. D., Trevisan, R., de Moraes, J. M., de Barros Ferraz, S. F., Villani, J. P., Duarte-Neto, P. J., and  
Martinelli, L. A.: Land-use change in the Atlantic rainforest region: Consequences for the hydrology of small catchments, *J.*  
1045 *Hydrol. (Amst.)*, 499, 100–109, <https://doi.org/10.1016/j.jhydrol.2013.06.049>, 2013.
- Scanlon, T. M. and Kustas, W. P.: Partitioning carbon dioxide and water vapor fluxes using correlation analysis, *Agric. For.*  
*Meteorol.*, 150, 89–99, <https://doi.org/10.1016/j.agrformet.2009.09.005>, 2010.
- Scanlon, T. M. and Kustas, W. P.: Partitioning Evapotranspiration Using an Eddy Covariance-Based Technique: Improved  
Assessment of Soil Moisture and Land–Atmosphere Exchange Dynamics, *Vadose Zone Journal*, 11,  
1050 <https://doi.org/10.2136/vzj2012.0025>, 2012.
- Scanlon, T. M. and Sahu, P.: On the correlation structure of water vapor and carbon dioxide in the atmospheric surface layer:  
A basis for flux partitioning, *Water Resour. Res.*, 44, <https://doi.org/10.1029/2008WR006932>, 2008.
- Scanlon, T. M., Schmidt, D. F., and Skaggs, T. H.: Correlation-based flux partitioning of water vapor and carbon dioxide  
fluxes: Method simplification and estimation of canopy water use efficiency, *Agric. For. Meteorol.*, 279,  
1055 <https://doi.org/10.1016/j.agrformet.2019.107732>, 2019.
- Schlesinger, W. H. and Jasechko, S.: Transpiration in the global water cycle, *Agric. For. Meteorol.*, 189–190, 115–117,  
<https://doi.org/10.1016/j.agrformet.2014.01.011>, 2014.
- Schreiner-McGraw, A. P., Ajami, H., Anderson, R. G., and Wang, D.: Integrating partitioned evapotranspiration data into  
hydrologic models: Vegetation parameterization and uncertainty quantification of simulated plant water use, *Hydrol. Process.*,  
1060 36, <https://doi.org/10.1002/hyp.14580>, 2022.



- Scott, R. L. and Biederman, J. A.: Partitioning evapotranspiration using long-term carbon dioxide and water vapor fluxes, *Geophys. Res. Lett.*, 44, 6833–6840, <https://doi.org/10.1002/2017GL074324>, 2017.
- Scott, R. L., Huxman, T. E., Cable, W. L., and Emmerich, W. E.: Partitioning of evapotranspiration and its relation to carbon dioxide exchange in a Chihuahuan Desert shrubland, *Hydrol. Process.*, 20, 3227–3243, <https://doi.org/10.1002/hyp.6329>, 1065 2006.
- Scott, R. L., Knowles, J. F., Nelson, J. A., Gentine, P., Li, X., Barron-Gafford, G., Bryant, R., and Biederman, J. A.: Water Availability Impacts on Evapotranspiration Partitioning, *Agric. For. Meteorol.*, 297, <https://doi.org/10.1016/j.agrformet.2020.108251>, 2021.
- Shih, C. H., Anderson, R. G., Skaggs, T. H., Juang, J. Y., Chen, Y. Y., Jang, Y. S., Gu, R. Y., Huang, C. Y., and Lo, M. H.: Challenges and limitations of applying the flux variance similarity (FVS) method to partition evapotranspiration in a montane cloud forest, *Agric. For. Meteorol.*, 362, <https://doi.org/10.1016/j.agrformet.2025.110391>, 2025. 1070
- Shuttleworth, W. J. and Wallace, J. S.: Evaporation from sparse crops-an energy combination theory, *Quart. I. R. Met. Soc.*, 111, 839–855, 1985.
- Shveytser, V., Stoy, P. C., Butterworth, B. J., Wiesner, S., Skaggs, T., Murphy, B., Wutzler, T., El-Madany, T. S., and Desai, A. R.: Evaporation and transpiration from multiple proximal forests and wetlands, <https://doi.org/10.1002/essoar.10511759.1>, 1075 5 July 2022.
- Siddiq, Z. and Cao, K. F.: Nocturnal transpiration in 18 broadleaf timber species under a tropical seasonal climate, *For. Ecol. Manage.*, 418, 47–54, <https://doi.org/10.1016/j.foreco.2017.12.043>, 2018.
- Sinclair, T. R., Tanner, C. B., and Bennett, J. M.: Water-Use Efficiency in Crop Production, *Bioscience*, 34, 36–40, 1080 <https://doi.org/10.2307/1309424>, 1984.
- Skaggs, T. H., Anderson, R. G., Alfieri, J. G., Scanlon, T. M., and Kustas, W. P.: Fluxpart: Open source software for partitioning carbon dioxide and water vapor fluxes, *Agric. For. Meteorol.*, 253–254, 218–224, <https://doi.org/10.1016/j.agrformet.2018.02.019>, 2018.
- Song, L., Liu, S., Kustas, W. P., Nieto, H., Sun, L., Xu, Z., Skaggs, T. H., Yang, Y., Ma, M., Xu, T., Tang, X., and Li, Q.: 1085 Monitoring and validating spatially and temporally continuous daily evaporation and transpiration at river basin scale, *Remote Sens. Environ.*, 219, 72–88, <https://doi.org/10.1016/j.rse.2018.10.002>, 2018.
- Song, L., Bateni, S. M., Xu, Y., Xu, T., He, X., Ki, S. J., Liu, S., Ma, M., and Yang, Y.: Reconstruction of remotely sensed daily evapotranspiration data in cloudy-sky conditions, *Agric. Water Manag.*, 255, <https://doi.org/10.1016/j.agwat.2021.107000>, 2021.
- 1090 Song, L., Ding, Z., Kustas, W. P., Xu, Y., Zhao, G., Liu, S., Ma, M., Xue, K., Bai, Y., and Xu, Z.: Applications of a thermal-based two-source energy balance model coupled to surface soil moisture, *Remote Sens. Environ.*, 271, <https://doi.org/10.1016/j.rse.2022.112923>, 2022.



- Song, L., Xu, Y., Liddell, M., Cui, Y., Liu, S., and Xu, P.: Application of a two source energy balance model coupled with satellite based soil moisture and thermal infrared data, *ISPRS Journal of Photogrammetry and Remote Sensing*, 204, 15–26, 1095 <https://doi.org/10.1016/j.isprsjprs.2023.08.009>, 2023a.
- Song, L., Ding, Z., Kustas, W. P., Hua, W., Liu, X., Liu, L., Liu, S., Ma, M., Bai, Y., and Xu, Z.: Applications of a Thermal-Based Two-Source Energy Balance Model Coupling the Sun-Induced Chlorophyll Fluorescence Data, *IEEE Geoscience and Remote Sensing Letters*, 20, <https://doi.org/10.1109/LGRS.2023.3240996>, 2023b.
- Stapleton, A., Eichelmann, E., and Roantree, M.: A framework for constructing machine learning models with feature set 1100 optimisation for evapotranspiration partitioning, *Applied Computing and Geosciences*, 16, 100105, <https://doi.org/10.1016/J.ACAGS.2022.100105>, 2022.
- Stoy, P. C., Katul, G. G., Siqueira, M. B. S., Juang, J. Y., Novick, K. A., Uebelherr, J. M., and Oren, R.: An evaluation of models for partitioning eddy covariance-measured net ecosystem exchange into photosynthesis and respiration, *Agric. For. Meteorol.*, 141, 2–18, <https://doi.org/10.1016/j.agrformet.2006.09.001>, 2006.
- 1105 Stoy, P. C., El-Madany, T. S., Fisher, J. B., Gentine, P., Gerken, T., Good, S. P., Klosterhalfen, A., Liu, S., Miralles, D. G., Perez-Priego, O., Rigden, A. J., Skaggs, T. H., Wohlfahrt, G., Anderson, R. G., Coenders-Gerrits, A. M. J., Jung, M., Maes, W. H., Mammarella, I., Mauder, M., Migliavacca, M., Nelson, J. A., Poyatos, R., Reichstein, M., Scott, R. L., and Wolf, S.: Reviews and syntheses: Turning the challenges of partitioning ecosystem evaporation and transpiration into opportunities, *Biogeosciences*, 16, 3747–3775, <https://doi.org/10.5194/bg-16-3747-2019>, 2019.
- 1110 Sulman, B. N., Roman, D. T., Scanlon, T. M., Wang, L., and Novick, K. A.: Comparing methods for partitioning a decade of carbon dioxide and water vapor fluxes in a temperate forest, *Agric. For. Meteorol.*, 226–227, 229–245, <https://doi.org/10.1016/j.agrformet.2016.06.002>, 2016.
- Sun, J. ying, Sun, X. yang, Hu, Z. yong, and Wang, G. xu: Exploring the influence of environmental factors in partitioning evapotranspiration along an elevation gradient on Mount Gongga, eastern edge of the Qinghai-Tibet Platea, China, *J. Mt. Sci.*, 1115 17, 384–396, <https://doi.org/10.1007/s11629-019-5687-1>, 2020.
- Sun, S. and Verseghy, D.: Introducing water-stressed shrubland into the Canadian Land Surface Scheme, *J. Hydrol. (Amst.)*, 579, <https://doi.org/10.1016/j.jhydrol.2019.124157>, 2019.
- Sun, Z., Zheng, Y., Li, X., Tian, Y., Han, F., Zhong, Y., Liu, J., and Zheng, C.: The Nexus of Water, Ecosystems, and Agriculture in Endorheic River Basins: A System Analysis Based on Integrated Ecohydrological Modeling, *Water Resour. 1120 Res.*, 54, 7534–7556, <https://doi.org/10.1029/2018WR023364>, 2018.
- Thomas, C., Martin, J. G., Goeckede, M., Siqueira, M. B., Foken, T., Law, B. E., Loescher, H. W., and Katul, G.: Estimating daytime subcanopy respiration from conditional sampling methods applied to multi-scalar high frequency turbulence time series, *Agric. For. Meteorol.*, 148, 1210–1229, <https://doi.org/10.1016/j.agrformet.2008.03.002>, 2008.
- Thomas, C. K., Martin, J. G., Law, B. E., and Davis, K.: Toward biologically meaningful net carbon exchange estimates for 1125 tall, dense canopies: Multi-level eddy covariance observations and canopy coupling regimes in a mature Douglas-fir forest in Oregon, *Agric. For. Meteorol.*, 173, 14–27, <https://doi.org/10.1016/j.agrformet.2013.01.001>, 2013.



- Tong, Y., Wang, P., Li, X. Y., Wang, L., Wu, X., Shi, F., Bai, Y., Li, E., Wang, J., and Wang, Y.: Seasonality of the Transpiration Fraction and Its Controls Across Typical Ecosystems Within the Heihe River Basin, *Journal of Geophysical Research: Atmospheres*, 124, 1277–1291, <https://doi.org/10.1029/2018JD029680>, 2019.
- 1130 Wagle, P., Skaggs, T. H., Gowda, P. H., Northup, B. K., and Neel, J. P. S.: Flux variance similarity-based partitioning of evapotranspiration over a rainfed alfalfa field using high frequency eddy covariance data, *Agric. For. Meteorol.*, 285–286, <https://doi.org/10.1016/j.agrformet.2020.107907>, 2020.
- Wagle, P., Gowda, P. H., Northup, B. K., and Neel, J. P. S.: Ecosystem-level water use efficiency and evapotranspiration partitioning in conventional till and no-till rainfed canola, *Agric. Water Manag.*, 250, <https://doi.org/10.1016/j.agwat.2021.106825>, 2021a.
- 1135 Wagle, P., Skaggs, T. H., Gowda, P. H., Northup, B. K., Neel, J. P. S., and Anderson, R. G.: Evaluation of Water Use Efficiency Algorithms for Flux Variance Similarity-Based Evapotranspiration Partitioning in C3 and C4 Grain Crops, *Water Resour. Res.*, 57, <https://doi.org/10.1029/2020WR028866>, 2021b.
- Wagle, P., Raghav, P., Kumar, M., and Gunter, S. A.: Influence of water use efficiency parameterizations on flux variance similarity-based partitioning of evapotranspiration, *Agric. For. Meteorol.*, 328, <https://doi.org/10.1016/j.agrformet.2022.109254>, 2023.
- 1140 Wang, L., Caylor, K. K., Villegas, J. C., Barron-Gafford, G. A., Breshears, D. D., and Huxman, T. E.: Partitioning evapotranspiration across gradients of woody plant cover: Assessment of a stable isotope technique, *Geophys. Res. Lett.*, 37, <https://doi.org/10.1029/2010GL043228>, 2010.
- 1145 Wang, L., Good, S. P., and Caylor, K. K.: Global synthesis of vegetation control on evapotranspiration partitioning, *Geophys. Res. Lett.*, 41, 6753–6757, <https://doi.org/10.1002/2014GL061439>, 2014.
- Wang, L., Liu, H., and Bernhofer, C.: Grazing intensity effects on the partitioning of evapotranspiration in the semiarid typical steppe ecosystems in Inner Mongolia, *International Journal of Climatology*, 36, 4130–4140, <https://doi.org/10.1002/joc.4622>, 2016a.
- 1150 Wang, L., Li, Y., Zhang, X., Chen, K., and Siddique, K. H. M.: Soil water content and vapor pressure deficit affect ecosystem water use efficiency through different pathways, *J. Hydrol. (Amst.)*, 640, <https://doi.org/10.1016/j.jhydrol.2024.131732>, 2024a.
- Wang, W., Smith, J. A., Ramamurthy, P., Baeck, M. L., Bou-Zeid, E., and Scanlon, T. M.: On the correlation of water vapor and CO<sub>2</sub>: Application to flux partitioning of evapotranspiration, *Water Resour. Res.*, 52, 9452–9469, <https://doi.org/10.1002/2015WR018161>, 2016b.
- 1155 Wang, X., Blanken, P. D., Kasemsap, P., Petchprayoon, P., Thaler, P., Nouvellon, Y., Gay, F., Chidthaisong, A., Sanwangsri, M., Chayawat, C., Chantuma, P., Sathornkich, J., Kaewthongrach, R., Satakhun, D., and Phattaralerphong, J.: Carbon and Water Cycling in Two Rubber Plantations and a Natural Forest in Mainland Southeast Asia, *J. Geophys. Res. Biogeosci.*, 127, <https://doi.org/10.1029/2022JG006840>, 2022.



- 1160 Wang, X., Zhou, Y., Huang, H., Gao, X., Sun, S., Meng, P., and Zhang, J.: Comparing Four Evapotranspiration Partitioning Methods from Eddy Covariance Considering Turbulent Mixing in a Poplar Plantation, *Water (Switzerland)*, 16, <https://doi.org/10.3390/w16111548>, 2024b.
- Wang, X., Li, Z., Zhou, Y., Wang, Y., Ahmad, S., Hu, M., Sun, S., Huang, H., Zhang, J., and Zhai, L.: Evaluation of water use efficiency model in evapotranspiration partitioning from high-frequency eddy covariance data - a comparison between  
1165 plantation sites, *Agric. For. Meteorol.*, 372, <https://doi.org/10.1016/j.agrformet.2025.110663>, 2025.
- Wang, Y., Cai, H., Yu, L., Peng, X., Xu, J., and Wang, X.: Evapotranspiration partitioning and crop coefficient of maize in dry semi-humid climate regime, *Agric. Water Manag.*, 236, <https://doi.org/10.1016/j.agwat.2020.106164>, 2020.
- Wang, Y., Anderegg, W. R. L., Venturas, M. D., Trugman, A. T., Yu, K., and Frankenberg, C.: Optimization theory explains nighttime stomatal responses, *New Phytologist*, 230, 1550–1561, <https://doi.org/10.1111/nph.17267>, 2021.
- 1170 Wang-Erlandsson, L., Van Der Ent, R. J., Gordon, L. J., and Savenije, H. H. G.: Contrasting roles of interception and transpiration in the hydrological cycle - Part 1: Temporal characteristics over land, *Earth System Dynamics*, 5, 441–469, <https://doi.org/10.5194/esd-5-441-2014>, 2014.
- Wei, Z., Yoshimura, K., Okazaki, A., Kim, W., Liu, Z., and Yokoi, M.: Partitioning of evapotranspiration using high-frequency water vapor isotopic measurement over a rice paddy field, *Water Resour. Res.*, 51, 3716–3729,  
1175 <https://doi.org/10.1002/2014WR016737>, 2015.
- Wei, Z., Yoshimura, K., Wang, L., Miralles, D. G., Jasechko, S., and Lee, X.: Revisiting the contribution of transpiration to global terrestrial evapotranspiration, *Geophys. Res. Lett.*, 44, 2792–2801, <https://doi.org/10.1002/2016GL072235>, 2017.
- Wilcox, B. P., Turnbull, L., Young, M. H., Williams, C. J., Ravi, S., Seyfried, M. S., Bowling, D. R., Scott, R. L., Germino, M. J., Caldwell, T. G., and Wainwright, J.: Invasion of shrublands by exotic grasses: Ecohydrological consequences in cold  
1180 versus warm deserts, *Ecohydrology*, 5, 160–173, <https://doi.org/10.1002/eco.247>, 2012.
- Williams, M., Richardson, A. D., Reichstein, M., Stoy, P. C., Peylin, P., Verbeeck, H., Carvalhais, N., Jung, M., Hollinger, D. Y., Kattge, J., Leuning, R., Luo, Y., Tomelleri, E., Trudinger, C. M., and Wang, Y.-P.: Improving land surface models with FLUXNET data, *Biogeosciences*, 1341–1359 pp., 2009.
- Wilson, K. B., Hanson, P. J., Mulholland, P. J., Baldocchi, D. D., and Wullschleger, S. D.: A comparison of methods for  
1185 determining forest evapotranspiration and its components: sap-flow, soil water budget, eddy covariance and catchment water balance, *Agricultural and Forest Meteorology*, 153–168 pp., 2001.
- Wolf, S., Paul-Limoges, E., Sayler, D., and Kirchner, J. W.: Dynamics of evapotranspiration from concurrent above- and below-canopy flux measurements in a montane Sierra Nevada forest, *Agric. For. Meteorol.*, 346, <https://doi.org/10.1016/j.agrformet.2023.109864>, 2024.
- 1190 Wu, Y. and Wang, P.: Decadal Dynamics of Energy Balance and Transpiration Fraction in an Alpine Ecosystem: A Modelling and Observational Study, *Ecohydrology*, 18, <https://doi.org/10.1002/eco.70029>, 2025.



- Xu, C., Zhu, G., Zhang, Y., and Che, T.: Partitioning of Evapotranspiration and Its Response to Eco-Environmental Factors Over an Alpine Grassland on the Qinghai–Tibetan Plateau Based on the SiB2 Model, *Hydrol. Process.*, 38, <https://doi.org/10.1002/hyp.15295>, 2024.
- 1195 Xu, Z., Zhu, Z., Liu, S., Song, L., Wang, X., Zhou, S., Yang, X., and Xu, T.: Evapotranspiration partitioning for multiple ecosystems within a dryland watershed: Seasonal variations and controlling factors, *J. Hydrol. (Amst.)*, 598, <https://doi.org/10.1016/j.jhydrol.2021.126483>, 2021.
- Xue, B., Wang, G., Xiao, J., Tan, Q., Shrestha, S., Sun, W., and Liu, T.: Global evapotranspiration hiatus explained by vegetation structural and physiological controls, *Ecol. Eng.*, 158, <https://doi.org/10.1016/j.ecoleng.2020.106046>, 2020.
- 1200 Xue, K., Song, L., Xu, Y., Liu, S., Zhao, G., Tao, S., Magliulo, E., Manco, A., Liddell, M., Wohlfahrt, G., Varlagin, A., Montagnani, L., Woodgate, W., Loubet, B., and Zhao, L.: Estimating ecosystem evaporation and transpiration using a soil moisture coupled two-source energy balance model across FLUXNET sites, *Agric. For. Meteorol.*, 337, <https://doi.org/10.1016/j.agrformet.2023.109513>, 2023.
- Yang, C., Lei, H., Hu, X., and Liu, M.: Development of an ecohydrological model for coupled simulation of water and carbon  
1205 fluxes, crop growth, and canopy spectra over croplands, *Comput. Electron. Agric.*, 235, <https://doi.org/10.1016/j.compag.2025.110336>, 2025a.
- Yang, S., Zhang, J., Han, J., Bai, Y., Xun, L., Zhang, S., Cao, D., and Wang, J.: The ratio of transpiration to evapotranspiration dominates ecosystem water use efficiency response to drought, *Agric. For. Meteorol.*, 363, <https://doi.org/10.1016/j.agrformet.2025.110423>, 2025b.
- 1210 Yu, L., Zhou, S., Zhao, X., Gao, X., Jiang, K., Zhang, B., Cheng, L., Song, X., and Siddique, K. H. M.: Evapotranspiration Partitioning Based on Leaf and Ecosystem Water Use Efficiency, *Water Resour. Res.*, 58, <https://doi.org/10.1029/2021WR030629>, 2022.
- Yuan, R., Chang, L., and Niu, G.: Annual variations of T/ET in a semi-arid region: Implications of plant water use strategies, *J. Hydrol. (Amst.)*, 603, <https://doi.org/10.1016/j.jhydrol.2021.126884>, 2021.
- 1215 Yuan, W., Zheng, Y., Piao, S., Ciais, P., Lombardozzi, D., Wang, Y., Ryu, Y., Chen, G., Dong, W., Hu, Z., Jain, A. K., Jiang, C., Kato, E., Li, S., Lienert, S., Liu, S., Nabel, J. E. M. S., Qin, Z., Quine, T., Sitch, S., Smith, W. K., Wang, F., Wu, C., Xiao, Z., and Yang, S.: Increased atmospheric vapor pressure deficit reduces global vegetation growth, 2019.
- Zahn, E. and Bou-Zeid, E.: Observational partitioning of water and CO<sub>2</sub> fluxes at National Ecological Observatory Network (NEON) sites: A 5-year dataset of soil and plant components for spatial and temporal analysis, *Earth Syst. Sci. Data*, 16, 5603–  
1220 5624, <https://doi.org/10.5194/essd-16-5603-2024>, 2024.
- Zahn, E., Bou-Zeid, E., Good, S. P., Katul, G. G., Thomas, C. K., Ghannam, K., Smith, J. A., Chamecki, M., Dias, N. L., Fuentes, J. D., Alfieri, J. G., Kwon, H., Caylor, K. K., Gao, Z., Soderberg, K., Bambach, N. E., Hipps, L. E., Prueger, J. H., and Kustas, W. P.: Direct partitioning of eddy-covariance water and carbon dioxide fluxes into ground and plant components, *Agric. For. Meteorol.*, 315, <https://doi.org/10.1016/j.agrformet.2021.108790>, 2022.



- 1225 Zahn, E., Ghannam, K., Chamecki, M., Moene, A. F., Kustas, W. P., Good, S., and Bou-Zeid, E.: Numerical Investigation of Observational Flux Partitioning Methods for Water Vapor and Carbon Dioxide, *J. Geophys. Res. Biogeosci.*, 129, <https://doi.org/10.1029/2024JG008025>, 2024.
- Zeng, Z., Piao, S., Li, L. Z. X., Wang, T., Ciais, P., Lian, X. U., Yang, Y., Mao, J., Shi, X., and Myneni, R. B.: Impact of Earth Greening on the Terrestrial Water Cycle, <https://doi.org/10.1175/JCLI-D-17-0236.s1>, 2018.
- 1230 Zeppel, M., Tissue, D., Taylor, D., MacInnis-Ng, C., and Eamus, D.: Rates of nocturnal transpiration in two evergreen temperate woodland species with differing water-use strategies, *Tree Physiol.*, 30, 988–1000, <https://doi.org/10.1093/treephys/tpq053>, 2010.
- Zhang, J., Yang, S., Wang, J., Zeng, R., Zhang, S., Bai, Y., and Zhang, J.: Evapotranspiration Partitioning for Croplands Based on Eddy Covariance Measurements and Machine Learning Models, *Agronomy*, 15, <https://doi.org/10.3390/agronomy15030512>, 2025a.
- 1235 Zhang, Q., Feng, Q., Su, Y., and Jian, C.: Evapotranspiration Partitioning of the *Populus euphratica* Forest Ecosystem in the Drylands of Northwestern China, *Plants*, 14, <https://doi.org/10.3390/plants14050680>, 2025b.
- Zheng, C., Wang, S., Chen, J. M., Xiao, J., Chen, J., Zhu, K., and Sun, L.: Modeling transpiration using solar-induced chlorophyll fluorescence and photochemical reflectance index synergistically in a closed-canopy winter wheat ecosystem, *Remote Sens. Environ.*, 302, <https://doi.org/10.1016/j.rse.2023.113981>, 2024.
- 1240 Zheng, C., Wang, S., Chen, J. M., Xiao, J., Chen, J., Zhang, Z., and Forzieri, G.: Estimating global transpiration from TROPOMI SIF with angular normalization and separation for sunlit and shaded leaves, *Remote Sens. Environ.*, 319, <https://doi.org/10.1016/j.rse.2024.114586>, 2025.
- Zhong, F., Jiang, S., Van Dijk, A. I. J. M., Ren, L., Schellekens, J., and Miralles, D. G.: Revisiting large-scale interception patterns constrained by a synthesis of global experimental data, *Hydrol. Earth Syst. Sci.*, 26, 5647–5667, <https://doi.org/10.5194/hess-26-5647-2022>, 2022.
- 1245 Zhou, S., Yu, B., Huang, Y., and Wang, G.: The effect of vapor pressure deficit on water use efficiency at the subdaily time scale, *Geophys. Res. Lett.*, 41, 5005–5013, <https://doi.org/10.1002/2014GL060741>, 2014.
- Zhou, S., Yu, B., Zhang, Y., Huang, Y., and Wang, G.: Partitioning evapotranspiration based on the concept of underlying water use efficiency, *Water Resour. Res.*, 52, 1160–1175, <https://doi.org/10.1002/2015WR017766>, 2016.
- 1250 Zhou, S., Yu, B., Zhang, Y., Huang, Y., and Wang, G.: Water use efficiency and evapotranspiration partitioning for three typical ecosystems in the Heihe River Basin, northwestern China, *Agric. For. Meteorol.*, 253–254, 261–273, <https://doi.org/10.1016/j.agrformet.2018.02.002>, 2018.
- Zwieback, S., Chang, Q., Marsh, P., and Berg, A.: Shrub tundra ecohydrology: Rainfall interception is a major component of the water balance, *Environmental Research Letters*, 14, <https://doi.org/10.1088/1748-9326/ab1049>, 2019.